minerals

Review

Evolution, Magmatic Source and Metallogenesis of A-Type Granites in the Fanchang Volcanic Basin, Middle and Lower Yangtze Metallogenic Belt: A Review

Songsong Zhang [1,2], Xiaoyong Yang [1,*] and Lei Liu [3,*]

1 School of Earth and Space Sciences, China University of Science and Technology, Hefei 230001, China; zss2087@163.com
2 Geological Survey of Anhui Province, Hefei 230001, China
3 Key Laboratory of Metallogenic Prediction of Nonferrous Metals and Geological Environment Monitoring, Ministry of Education, School of Geosciences and Info-Physics, Central South University, Changsha 410083, China
* Correspondence: xyyang@ustc.edu.cn (X.Y.); liu01@ustc.edu.cn (L.L.)

Abstract: The Fanchang volcanic basin (FVB) is located in the Middle and Lower Yangtze Metallogenic Belt (MLYMB) between the ore districts of Ningwu and Tongling. The existing ore deposits in the FVB are relatively small in scale and related to late Mesozoic A-type granites. In this paper, the crystallization age, major and trace element composition, and Sr-Nd and Hf isotope compositions of the A-type granites are summarized from the literature; in addition, the magnetite composition, H and O isotopes of fluid inclusions, and sulfur isotope composition of metal sulfides in some typical ore deposits in the FVB are also summarized to give insights into the petrogenesis and mineralization of the A-type granites intruding into the FVB. The results show that: (1) Orthopyroxene, plagioclase, K-feldspar, and biotite are the main fractionating minerals controlling the evolution of the magmas of A-type granites in the FVB and other areas in the MLYMB. (2) The whole-rock Sr-Nd and zircon Hf isotopic characteristics show that the source of A-type granite magma is complex and includes the enriched mantle, lower crust, and upper crust, probably with stronger participation of Archaean–Paleoproterozoic crustal materials in the FVB granites than in other regions of the MLYMB. (3) The ores in the FVB are dominated by skarn and hydrothermal deposits. H and O isotopes of fluid inclusions indicate that ore-forming fluids have been derived from mixtures of magmatic hydrothermal fluid, meteoric waters, and deep brine related to gypsum layers. S isotopes of metal sulfides indicate that the sulfur may be a mixture of magmatically derived sulfur and sulfur originating from the Triassic gypsum-bearing layers. The deposit and ore characteristics of the main deposits in the FVB are also illustrated, and the evaluation of metal resources indicates that the skarn and hydrothermal iron–zinc ores in the FVB also have potential as sources of Cd, Ga, and Se. In addition, in terms of the oxygen fugacity, rock type, and geochemical characteristics of magmatic rocks, the metallogenic characteristics and potential of the A-type granites in the FVB are evaluated. It is considered that in addition to the dominant constituents of iron and zinc and the minor constituents listed above, the FVB could have the potential for providing copper, gold, molybdenum, uranium, and other metals as well.

Keywords: Middle and Lower Yangtze Metallogenic Belt (MLYMB); Fanchang volcanic basin (FVB); A-type granite suite; magma source area; exploration potential

Citation: Zhang, S.; Yang, X.; Liu, L. Evolution, Magmatic Source and Metallogenesis of A-Type Granites in the Fanchang Volcanic Basin, Middle and Lower Yangtze Metallogenic Belt: A Review. *Minerals* **2023**, *13*, 571. https://doi.org/10.3390/min13040571

Academic Editor: Jaroslav Dostal

Received: 26 February 2023
Revised: 13 April 2023
Accepted: 16 April 2023
Published: 18 April 2023

1. Introduction

A-type granites, an important category of granites [1–17], are closely related to some key metals or strategic minerals, including iron, zinc, cobalt, tin, cadmium, niobium, gallium, cobalt, REE, uranium, etc. [18–30].

In the 1960s, with the advent of the theory of plate tectonics, the genesis of granite was mostly explained in its framework, and in the 1970s and 1980s, research on granite classification reached its peak [31–33]. Up to now, there have been about 20 genetic classification schemes for granites, among which the MISA classification based on the character of presumed source rocks is one of the more commonly used [34–37]. The classification of I-type (igneous source) and S-type (sedimentary source) is based on the study of the granites in the Berridale–Kosciuszko area of the Lachlan Fold Belt, Australia [31]. The model provides a good explanation for the appearance of these two types of granites and indicates that the unique compositional features of these granites were inherited from their source rocks [38].

Loiselle and Wones [33] first defined A-type granites as alkaline, anhydrous, and anorogenic granites, named after the initial letter "A" of the three words. The widespread use of the concept of A-type granite started with the determination of the granite complex in southeastern Australia, which is mainly characterized by high contents of Nb, Ga, Y, and REE and low contents of Al, Mg, and Ca [1]. Then, Whalen et al. [3] constructed discriminant diagrams for A-type granites as opposed to orogenic granites, based on the Ga/Al ratio, Zr, Nb, Ce, Y contents, and so forth.

At present, the concept of A-type granite contains a wide range of rock types, such as alkaline granites, quartz syenites, and charnockites [5,8,39]. The distinguishing geochemical indicators include high contents of $Na_2O + K_2O$, Y, Nb, REE, and Ga, as well as high FeO_T/MgO, K_2O/Na_2O, and Ga/Al ratios, and low contents of V, Cr, Ni, Sr, Ba, and large negative Eu anomalies, plus flat HREE partitioning characteristics [1,3,15,37,40]. So far, there has been no unified understanding of the genesis of A-type granites, and the main genetic models include magmatic differentiation or low-degree partial melting of mantle-derived tholeiitic magma, residual melt generated by the differentiation of mantle-derived alkaline magma, and partial melting of F-rich residue after partial melting to form I-type granite, as well as interaction between mantle-derived alkaline magma and crustal materials [1,3,5,7–10,14,16,17,19,22,26,40–48]. Regardless of the origin of A-type granites, however, it is generally believed that their formation temperatures are relatively high [13,37,42,43,45].

So far, there have been many classification schemes for A-type granites [8–10,49,50]. Eby [8] proposed discriminant diagrams corresponding to the tectonic environment, dividing A-type granites into two types: A1 and A2, based on their Nb/Y ratios. The former suggests a non-orogenic intraplate setting related to a continental rift environment or mantle hot spot, while the latter is attributed to a post-collision or post-orogenic environment. In addition, Hong et al. [49] divided A-type granites into two categories, i.e., non-orogenic (AA type) and post-orogenic (PA type), and Liu et al. [50] further discussed this classification. King et al. [10] also proposed the concept of aluminous A-type granite, and many Chinese scholars then carried out some further research work, including the division between metaluminous, aluminous, and peraluminous granites [51–53]. Nowadays, geologists have extended the concept even to extrusive rocks; still, the extensional system is the main tectonic environment for their formation, while the magmatic sources may be diverse [2,3,11,46].

Systematic studies on the relationship between the geochemical properties of granite (such as oxygen fugacity, etc.) and metallogenic types began in the early 1980s [54–56]. At present, scholars have obtained some understanding of the relationship between the differentiation degree of magmatic rocks, the redox state of the magma, and the dominant metallic mineral deposits of granite (such as Sn, W, Mo, Cu, and Au) [57–60]. For example, porphyry Cu and Mo deposits are mainly associated with I-type granites with high oxygen fugacity, tungsten mineralization can occur in any granite type, and tin mineralization is generally associated with heavily fractionated, reduced felsic granites [21,31,37,58,61,62].

Ores closely related to A-type granites include zinc, tin, molybdenum, bismuth, niobium, tungsten, thallium, REE, fluorine, and uranium [1,3,6,24,63–66], with different characteristics in different ore-forming belts. For example, in the Middle and Lower Yangtze

Metallogenic Belt (MLYMB), iron, zinc, gold, molybdenum, and uranium are generally dominant [23,67–72], while in South China, tin, tungsten, and REE mineralization are the main types [24,48,73,74].

There are two A-type granite belts that are parallelly and symmetrically distributed on both sides of the Yangtze River in the Anhui Province (Figures 1 and 2), within the MLYMB, in eastern China. The granite belt on the north bank stretches from the Dalongshan granite massif in the Anqing area to Chengshan and Huangmeijian in Zongyang County, in a NE direction, for about 75 km. On the south bank, the A-type granite belt extends from the granite massifs of Huayuangong and Maotan in the Guichi area to Banshiling and Fushan in the Fanchang volcanic basin (FVB), for about 100 km and in a NE direction as well [75,76].

The FVB is located between the Tongling and Ningwu ore fields (Figure 1B). The formation and evolution of the FVB is controlled by Mesozoic plate collision, intracontinental orogeny, and transtension processes. It is a volcanic basin superimposed on a Middle Triassic–Early and Middle Jurassic sedimentary basin [77], which is intruded by A-type granites. Compared with other areas in the MLYMB, the A-type granite suite in the FVB has unique ore characteristics, mainly because of its enrichment in iron and zinc [78–81].

The crystallization ages, petrogenesis, and evolution of the A-type granites in the FVB have been defined earlier based on the major and trace element geochemistry, zircon U-Pb dating, and whole-rock Sr-Nd isotope and zircon Hf isotope investigations [82–85]. However, there are two main issues that remain unresolved: (1) The contribution of mantle-derived materials to the A-type granite source has generally been recognized, but the end-member characteristics of the crustal components are still unclear. Lou et al. [82] believed that a mantle-derived alkaline basaltic magma interacted with a siliceous magma from the lower crust, and the resulting evolved magma in turn interacted with Meso-Neoproterozoic shallow metamorphic rocks and formed a shallow magma chamber, from which A-type granites evolved through separation and crystallization processes. Yan et al. [85,86] considered that A-type granites in this area were formed by a mixture of mantle-derived and crust-derived magma in different proportions, with crust-derived magma being the product of middle-upper crust melting. There has been no conclusion as to whether Archean–Paleoproteroic crustal materials have been involved. (2) The comparison in terms of magmatic evolution, petrogenesis, and ore-forming characteristics of A-type granites in the FVB with other A-type rocks in the MLYMB is insufficient; therefore, the similarities and differences between them are not clear, particularly when it comes to their geochemical characteristics [84,86].

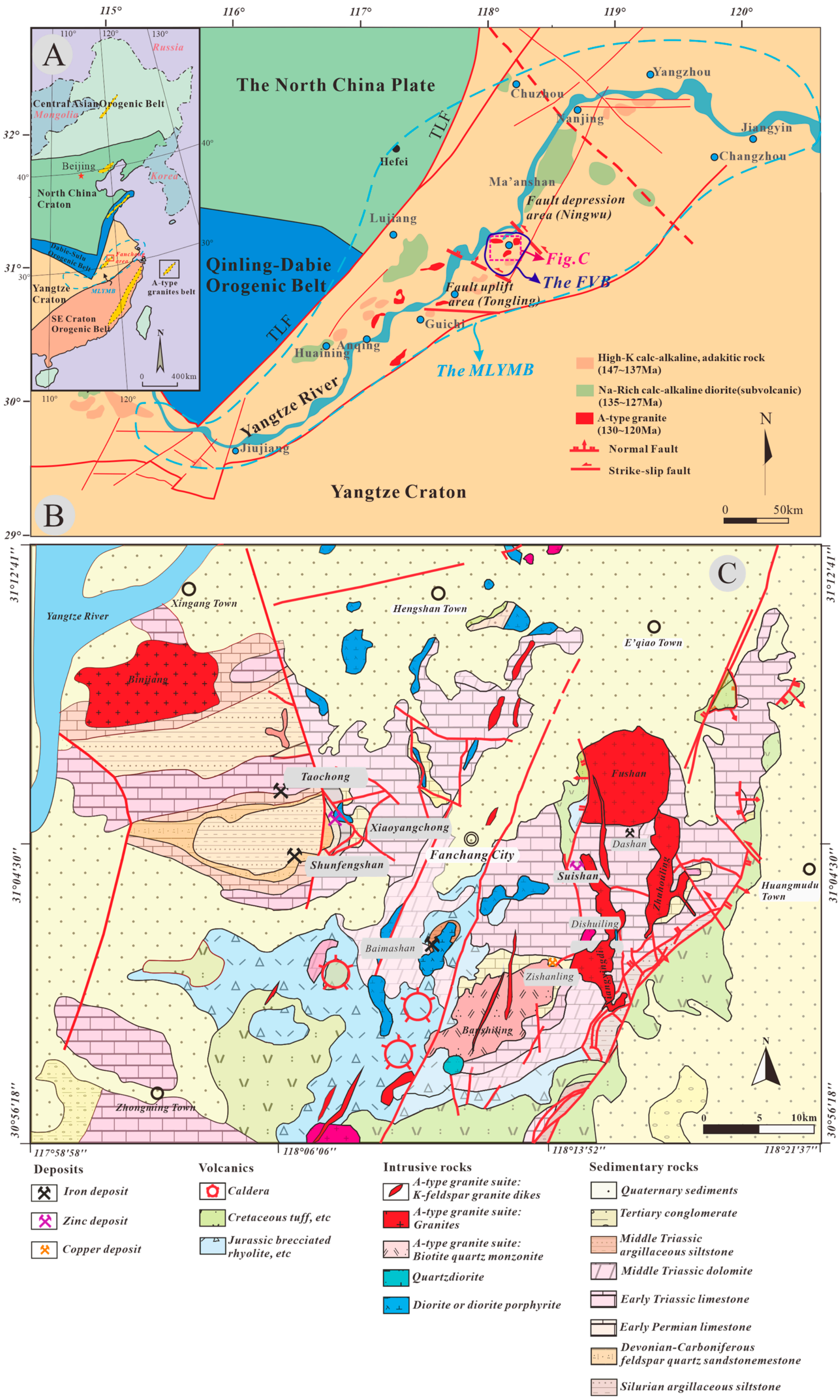

Figure 1. (**A**) Tectonic sketch map showing A-type granite belts in eastern China (modified from [76]); (**B**) sketch map showing the A-type granites of the MLYMB (modified from [72,87]); (**C**) main ore deposits related to the A-type granites of the FVB.

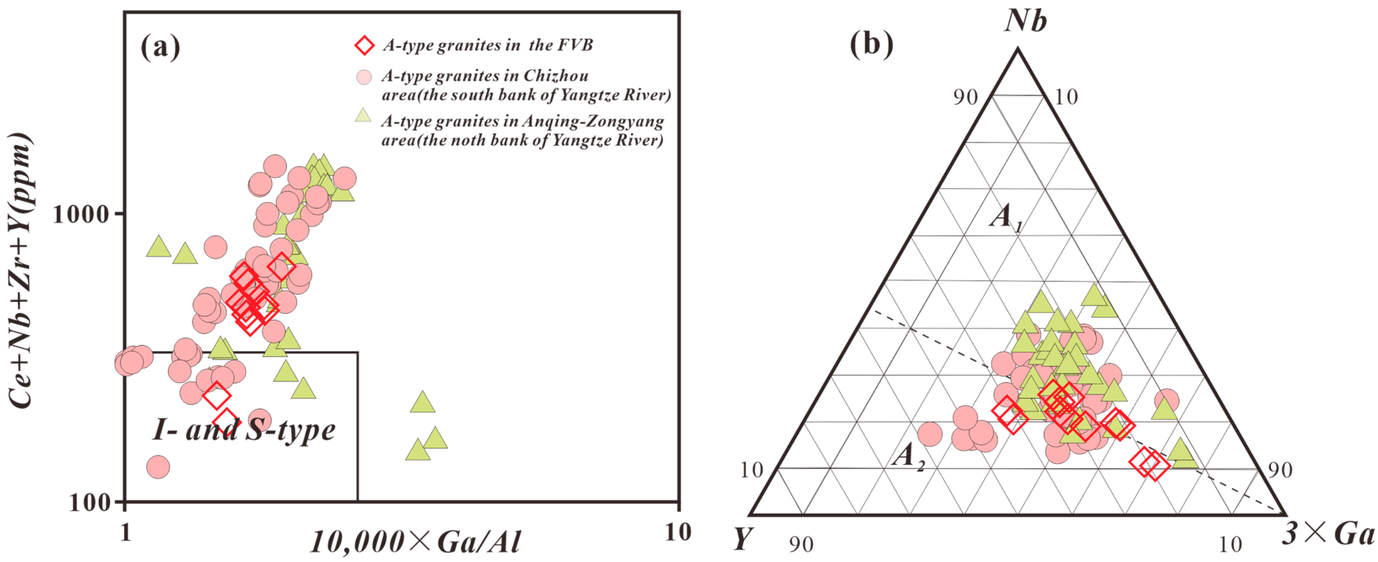

Figure 2. Discrimination diagrams of A-type granites in the MLYMB (figure (**a**) after [3] and (**b**) after [8]). Data sources: A-type granites in the FVB [46,82,85,88,89]; A-type granites in the Chizhou area (the south bank of the Yangtze River) [46,90–96]; A-type granites in the Anqing–Zongyang area (the north bank of the Yangtze River) [97–103].

Research on mineralization related to A-type granite in the MLYMB, such as ore types, ore-controlling characteristics, ore deposit genesis, etc., has not been systematically summarized before. This is especially so for the FVB, in which the dominant metals related to A-type granites are only iron and zinc, and deposits are relatively small [79–81,104–106]. Previous summaries on ore-forming types, deposit characteristics, and ore characteristics in this area are not thorough enough [78], and the discussion on the geochemistry of the deposits is still insufficient [80], in particular with respect to the characteristics of ore-forming fluid and the source of ore-forming materials. In addition, new breakthroughs have been carried out in this area, which makes it urgent to give insights into the metallogenic potential of the A-type granite suite and expand the list of prospective metals in this area.

In view of this, on the basis of the data on A-type granites in the MLYMB systematically collected and analyzed during the last few years, such as crystallization ages [46,83–85,89,92–94,96,98,100,101,107–109], major and trace elements [46,82,84,85,88,89,92–94,96,98,100,101,107,108], Sr-Nd [85,86,89,91,93,94,100,101,108,110,111], and Hf-O isotopes [85,88,92–94,96,100,112] (Table 1 and Supplement Tables S1–S4), this paper gives insights into the evolution characteristics of the A-type granite suite in the FVB and other parts of the MLYMB, as well as the end-member characteristics of the magma source area. Based on summaries of the characteristics of typical ore deposits related to A-type granites in the MLYMB [77,113], combined with the compositions of magnetite, H and O isotopes of fluid inclusions in ore and gangue minerals, as well as S isotopes of metal sulfides in typical deposits in the FVB (Supplement Tables S5–S7) [80,81], the ore-controlling factors, ore-forming fluids, and the sources of materials in the ores of the FVB are discussed. Based on the oxygen fugacity, rock types, and geochemical characteristics of magmatic rocks, this paper interprets the metallogenic potential of A-type granites in this area and expands their potential ore types. In addition, this paper preliminarily evaluates the comprehensive utilization potential of associated key metals in the main ores in the FVB, and finally, a petrogenic and metallogenic model for the A-type granite suite in the FVB is proposed.

Table 1. Summary of A-type granites in MLYMB.

No.	Area	Rock Massif	Location (Approximate Center)		Outcrop Area (km^2)	Lithology	Minerals		Sr-Nd		Hf-O		References
								Ages (Ma)	($^{87}Sr/^{86}Sr$)	εNd (t)	εHf (t)	$\delta^{18}O$‰	
1	Fanchang	Banshiling	30°59′59′′ N	118°11′06′′ E	16.29	Biotite quartz monzonite	Kfs (45%) + Pl (35%) + Qtz (10%) + Bt (6%)	125.3 ± 1.4	-	-	-	-	[46]
								124.9 ± 1. 7	0.7072	−6.8	−2.7~−6.3	6.7~7.4	[85,86]
								125.3 ± 2.9	-	-	-	-	[83]
								125.4 ± 1.6	0.70827	−11.2	-	-	[89]
2	Fanchang	Fushan	31°09′05′′ N	118°03′08′′ E	15.25	Syenogranite	Kfs (55%) + Qtz (30%) + Pl (5%) + Bt (5%)	124.9 ± 2.0	-	-	−5.8~−10.0	-	[88]
								126.8	-	-	−7.52	-	[84]
								126.4 ± 1.7	0.7076	−7.7	−1.6~7.9	7.1~9.1	[85,86]
3	Fanchang	Binjiang	31°09′05′′ N	118°03′08′′ E	12	Granitic porphyry	Kfs (60%) + Pl (20%) + Qz (15%) +Bt (5%)	124.3 ± 2.5	-	-	-	-	[83]
								124.6 ± 4.7 (coarse-grained granite)	0.7078	−3.4	0~−6.6	8.0~10.3	[85,86]
								123.0 ± 1.8 (granite porphyry)					
4	Fanchang	Xiangxingdi	31°02′00′′ N	118°15′30′′ E	6	Granitic porphyry	Qtz(25%) + Pl(70%) + Hb(2%)	124.3 ± 1.2	-	-	-	-	[89]
5	Fanchang	Suishan	31°05′00′′ N	118°12′00′′ E	-	Granite	Qtz(22%) +Pl(20%) + Kfs(53%) + Bt(4%)	124.3 ± 1.2	0.70755	−10.5	-	-	[89]
6	Fanchang	Zhuhouling	31°05′00′′ N	118°16′00′′ E	4.85	Granitic porphyry	Kfs(70~80%) + Qtz(<5%) + Pl(10~15%)	127.6 ± 1.8	0.70827	−11.2	-	-	[89]
7	Fanchang	Xiaoyang-chong	31°05′30′′ N	118°07′00′′ E	0.13	Quartz diorite and granodiorite	Kfs(15%) + Qtz(18~20%) + Pl(50~60%) + Bt(5~10%)	126~128	-	-	-	-	[113]
8	Chizhou	Huayuan-gong	117°36′00′′ N	30°37′00′′ E	220	Quartz syenite	Kfs(70~80%) + Qtz(<5%) + Pl(10%)	126.2 ± 1.2	0.7081	−6.7	−7.4	-	[93]
						Syenogranite	Kfs(64~67%) + Qtz(25~33%) + Pl(2.5~3.0%) + Bt(1.0%)	125.3 ± 1.2 [47]	–	-	−7.3, −7.89 [42]	-	[42,46]
						Quartz monzonite	Kfs(30~35%) + Qtz(5~10%) + Pl(45~55%) + Bt(3~6%) + Hb(2~4%)	127 ± 1	0.709776	−7.42	-	-	[108]
						Quartz syenite	Kfs(65~75%) + Qtz(5~10%) + Pl(7~9%) + Bt(1~3%) + Hb(1~4%)	127	0.713653	−7.67	-	-	[108]

Table 1. *Cont.*

No.	Area	Rock Massif	Location (Approximate Center)		Outcrop Area (km^2)	Lithology	Minerals	Sr-Nd			Hf-O		References
								Ages (Ma)	($^{87}Sr/^{86}Sr$)	εNd (t)	εHf (t)	$\delta^{18}O$‰	
						Syenogranite	Kfs(55~65%) + Qtz(5~10%) + Pl(2~5%) + Bt(1~2%)	127	0.740000	−7.97	-	-	[108]
						Syenogranite		122.6 ± 1.3	-	-	−4.7	-	[92]
						Syenogranite		122.6 ± 1.3	-	-	−6.7~−2.1	-	[94]
9	Chizhou	Bashan	117°38′00″ N	30°35′00″ E	40	Syenogranite	Kfs(66%) + Qtz(25%) + Pl(2%) + Ab(5%)	121.6 ± 2.8	0.7082~0.7091	−7.2~−7.5	-	-	[111]
10	Chizhou	Guilinzheng	117°40′00″ N	30°25′00″ E	-	Granitic porphyry	Kfs(40~60%) + Qtz(35~45%) + Pl(5~10%) + Bt(<5%)	127.0 ± 0.5 [94]; 127.6 ± 1.5 [114]	-	-	−2.9~5.9	-	[94,114]
11	Chizhou	Yangshan	117°50′00″N	30°30′00″ E	30	Syenitic porphyry	Kfs(40~45%) + Qtz(5~10%) + Pl(40~50%)	127.0 ± 0.6	0.7107~0.7140	−7.02~−5.78	−5.5~−3.7	-	[94]
						Syenogranitic porphyry	Kfs(30~35%) + Qtz(55~65%)	126.0 ± 1.0	0.7094~0.7065	−6.03~−5.47	−6.4~−4.4	-	[94]
						Syenogranite	-	127.6 ± 0.6	-	-	−7.5~−2.3	-	[94]
12	Chizhou	Maotan	117°47′00″ N	30°42′00″ E	25	Syenite	Kfs(55~65%) + Qtz(30%) + Pl(10%) + Bt(2~5%)	127.7 ± 1.8	0.70076	−7.03	-	-	[91]
						Syenogranite	Kfs(76~79%) + Qtz(7~22%) + Pl(1~4%) + Bt(0.5~3%)	125.4 ± 2.2	-	-	-	-	[46]
13	Chizhou	Xiangshui-jian	118°14′00″N	31°02′00″ E	20	Syenogranite	Kfs(64~67%) + Qtz(22~28%) + Pl(2~3%) + Bt(5~8%)	125.4 ± 1.4	-	-	-	-	[46]
14	Anqing-Guichi	Dalongshan	117°04′00″ N	30°36′00″ E	90	Quartz syenite	Kfs(60~70%) + Qtz(10~15%) + Pl(10~15%) + Bt(<5%)	125.8 ± 1.6, 126.4 ± 3.5 [112]; 123.8.4 ± 2.1 [84]	0.706444 [115]	−6.8~−7.7 [115]	−4~+1.1,−7.8~−3.6 [112]; −3.41 [84]	-	[84,112,115]
15	Anqing-Guichi	Huashan	117°09′00″ N	30°42′00″ E	21	Syenogranite	Kfs(70%) + Qtz(20%) + Pl(10%) + Bt(<5%)	126.2 ± 0.8; 124.4 ± 2.2	-	-	−3.51	-	[84]
16	Anqing-Guichi	Zongyang	117°14′00″ N	30°43′00″ E	10	Syenogranite	Kfs(70%) + Qtz(20%) + Pl(12%) + Bt(<1%)	124.8 ± 2.2 [98]; 125.4 ± 1.5 [84]	-	-	−3.57 [84]	-	[84,98]
17	Anqing-Guichi	Chengshan	117°14′00″ N	30°46′00″ E	19	Syenogranite	Kfs(70%) + Qtz(20%) + Pl(8%) + Aegirine(a small amount)	126.5 ± 2.1 [98] 125.0 ± 1.7 [84]	0.7076 [115]; 0.70695~0.70742 [101]	−5.0, −6.3~−4.2 [101]	−4.72 [84]	-	[84,98,101, 115]
18	Anqing-Guichi	Hejiaao	117°13′00″N	30°43′00″ E	5	Syenogranite	Kfs(75%) + Qtz(20%) + Pl(8%) + Ae(a small amount)	128 ± 1	0.70795~0.70931	−6.4~−5.8	-	-	[101]

Table 1. *Cont.*

No.	Area	Rock Massif	Location (Approximate Center)		Outcrop Area (km^2)	Lithology	Minerals	Sr-Nd			Hf-O		References
								Ages (Ma)	($^{87}Sr/^{86}Sr$)	εNd (t)	εHf (t)	$\delta^{18}O$‰	
19	Anqing-Guichi	Meilin	117°12′30′′ N	30°43′00′′ E	7	Syenogranite	Kfs(75%) + Qtz(20%) + Pl(5%) + Ae(a small amount)	128 ± 2	0.7364~0.7659	−5.2, −6.0, −5.4	-	-	[101]
20	Anqing-Guichi	Huangmeijian	117°34′00′′ N	30°55′30′′ E	120	Quartz syenite	Kfs(86%) + Qtz(12%) + Pl(<2%)	127.6 ± 2.1; 127.2 ± 2.1 [112]	0.7078 [115]; 0.7089 [110]	−7.7 [115]; −2.5 [110]	−3.3~+2.1 [112]; −3.8~−0.1 [112]; −3.38 [84]	-	[84,110,112,115,116]
21	Anqing-Guichi	Changgang	117°12′00′′ N	31°20′00′′ E	0.5	Syenogranitic porphyry	Kfs(45~55%) + Qtz(15~20%) + Pl(20~30%) + Bt(a small amount)	120 ± 2	0.7082	−14.9	−18.3	5.99	[100]

2. Geological Background of the Fanchang Volcanic Basin

According to the geological characteristics, mineral assemblages, and metallogenic ages of the deposits in the MLYMB, two metallogenic stages are distinguished: one related to Hercynian submarine eruptive volcano-sedimentary processes, and the other related to Yanshanian (Late Jurassic and Early Cretaceous) intermediate-acid intrusive rocks [117,118]. The metallogenic stage related to the Yanshanian intermediate-acid intrusive rocks is the most important and is connected to the thinning of the continental lithosphere in eastern China [67,71,72,117,119,120]. The Yanshanian metallogenic stages can be subdivided into three types (Figure 1B): (1) the skarn-porphyry Cu and Au mineralization associated with high-K calc-alkaline, adakitic rocks (147~137 Ma), mainly developed in Jiurui, Anqing-Guichi, Tongling (fault uplift area) [121–125], and the southeastern Hubei province in a transitional zone of fault depression and fault uplift [126–129]; (2) the subvolcanic or porphyrite-type Fe mineralization related to Na-rich calc-alkaline subvolcanic diorite (135–127 Ma), mainly developed in volcanic basins such as Ningwu and Luzong [107,130–132]; and (3) Fe, Au, Mo, and U mineralization related to alkaline or A-type granites (130–120 Ma), developed both in fault uplift areas and volcanic basins, mainly the FVB, Luzong volcanic basin, and the uplift area of Chizhou [67,69,72,118].

The FVB is a compound basin covered by Mesozoic volcanic rocks, which are superposed on an earlier fault-bounded basin [105,133], found between the fault uplift area (Tongling) and the volcanic basin (Ningwu) (Figure 1B). Late Mesozoic magmatic activity in the FVB was intense, and the volcanic rocks are mainly distributed in the southern part, whereas A-type granites are mainly found in the central and northern parts (Figure 1C).

Volcanic rocks are mainly distributed around Tadpole Mountain, Maren Mountain, and other craters, with a total thickness of between 220 and 2250 m. There are three eruptive cycles from bottom to top, namely the Kedoushan Formation, Chisha Formation, and Zhongfencun Formation, characterized by successive bimodal eruptions of basalt and rhyolite [113], dated between 129 and 131 Ma [134]. The crystallization time of the intrusive rocks is slightly later than that of the extrusive rocks, and they are dominated by A-type granites [75,89,135]. There are similar abundance patterns of trace elements (especially incompatible elements), Sr-Nd isotopes, and zircon Hf-O isotopes between the intrusive rocks and volcanic rocks in the FVB [85,90,134].

Previous studies have shown that the mantle endmember of the Yanshanian magmatic rocks in the MLYMB appears to be enriched [71,72,136–141]. On the other hand, crustal materials were also obviously involved during the petrogenetic process [122,142–147]. Our previous studies have also shown that the patterns of trace elements in the intrusive rocks in the FVB are similar to those in typical crustal rocks, indicating the participation of crustal materials during the formation of the A-type granites [83,89].

3. Evolution of the A-Type Granites in the FVB

The A-type granites in the FVB mainly belong to the high-K calc-alkaline and shoshonite suites (Figure 3a). They are mainly metaluminous and peraluminous (Figure 3c). Granites and quartz mozonites are the main rock types of A-type granites in the FVB (Figures 3b and 4d,e), followed by a few syenite and granodiorite rocks. The A-type granites in the FVB and MYLMB are enriched in light rare-earth elements with flat, heavy rare-earth element curves (Figure 3d). They are enriched in Rb, Th, U, Ce, Pb, Nd, Sm, and Gd, but depleted in Ba, Nb, Ta, Sr, P, and Ti, reflecting a trace element abundance pattern roughly consistent with the crust, with more marked peaks and troughs (Figure 3e). The crystallization age of Mesozoic intrusive rocks in the FVB is mainly between 128 and 123 Ma, which essentially overlaps with the crystallization ages of A-type granites in the rest of the MLYMB (Figure 3f).

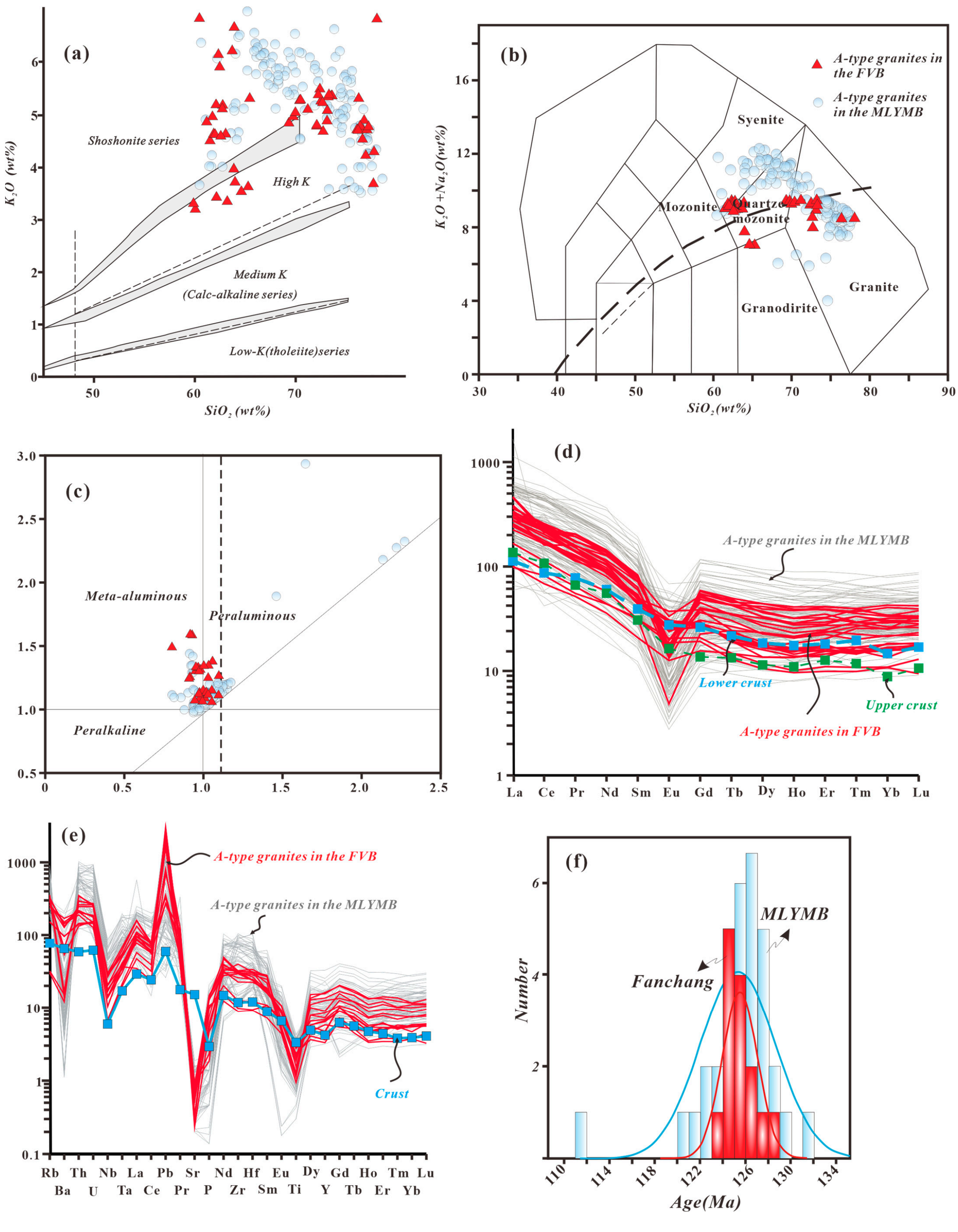

Figure 3. Some basic geochemical diagrams of A-type granites in the FVB and MYLMB. (**a**) K_2O vs. SiO_2 diagram (after [148]); (**b**) TAS diagram (after [149]); (**c**) A/NK vs. A/CNK diagram (after [148]); (**d**) chondrite-normalized rare earth element patterns (normalization values after [150]), data of the lower and upper crusts are from [151]; (**e**) primitive mantle-normalized trace element patterns (normalization values after [150]), crust data are from [152]; (**f**) crystallization ages. Data source (see Supplement Table S2): major and trace elements of A-type rocks in the FVB are from [46,82,85,88,89]; major and trace elements of A-type granites in other areas of the MLYMB are from [46,84,92–94,96,98,100,101,107,108]; and crystallization ages of A-type granites in the FVB and other parts of the MLYMB are from [46,83–85,89,92–94,96,98,100,101,107–109].

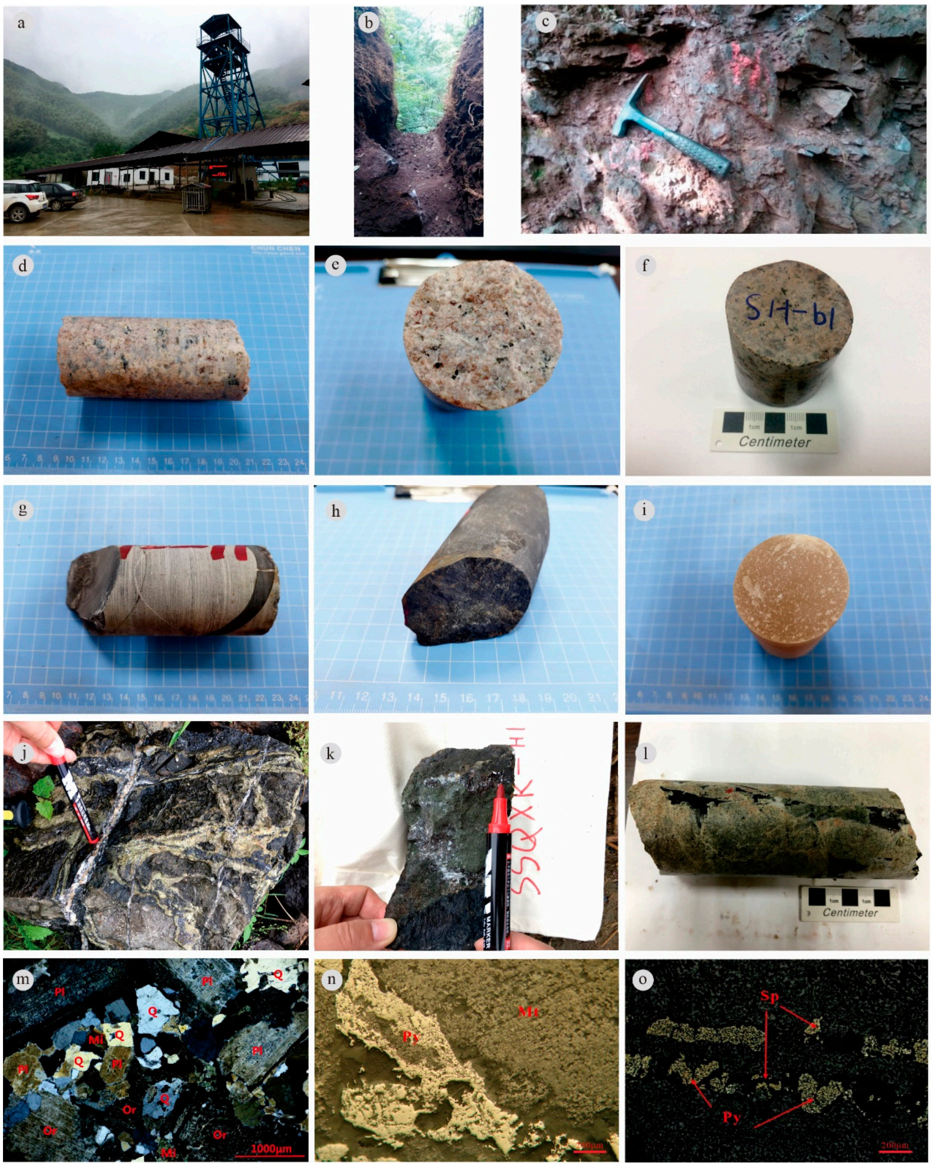

Figure 4. Photos of typical A-type granites and related ores in the FVB. (**a**) Xiaoyangchong mining area; (**b**) trench in Suishan mining area; (**c**) outcrop of hematitization skarn; (**d**,**e**) typical A-type granite in Taochong mining area; (**f**) typical A-type granite in Suishan mining area; (**g**–**i**) cores of main ore-bearing strata: g-banded limestone, h-siltstone, and i-anhydrite; (**j**–**l**) main ore types related to A-type granite: j-Xiaoyangchong skarn magnetite ore; k-Suishan hydrothermal magnetite-sphalerite ore; l-Suishan garnet skarn; (**m**) microphotograph (crossed nicols) of typical A-type granite; (**n**) reflected light photograph of magnetite ore; (**o**) reflected light photograph of pyrite–sphalerite ore.

The Harker diagram and trace element covariant diagram are used to investigate the magmatic evolution process. As can be seen from Figure 5, the intrusive rocks in the FVB are similar to other A-type granites in the MLYMB, and fractional crystallization plays a dominant role in the magmatic evolution process. According to the Harker diagram (Figure 6), SiO_2 content is negatively correlated with Fe_2O3_T, MgO, P_2O_5, and TiO_2 content, indicating the separation and crystallization of Fe-bearing mafic minerals (pyroxene, amphibole, and biotite), apatite, and titanite. The negative correlation with Al_2O_3, CaO, and Eu/Eu* indicates the crystallization of plagioclase.

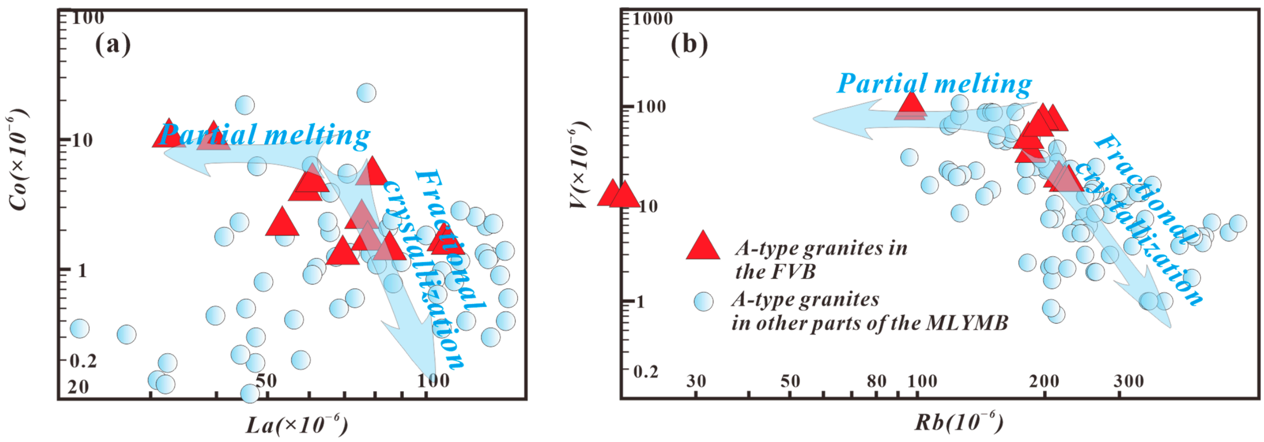

Figure 5. Log–log diagrams of compatible elements' content vs. incompatible elements' content of A-type granites in the FVB and other areas in the MLYMB (after [153]): (**a**) Co vs. La; (**b**) V vs. Rb. Data sources (see Supplement Table S1): A-type granites in the FVB are from [46,82,85,88,89]; other areas in the MLYMB are from [46,84,92–94,96,98,100,101,107,108]. Data sources of Figures 6–8 are the same as Figure 5.

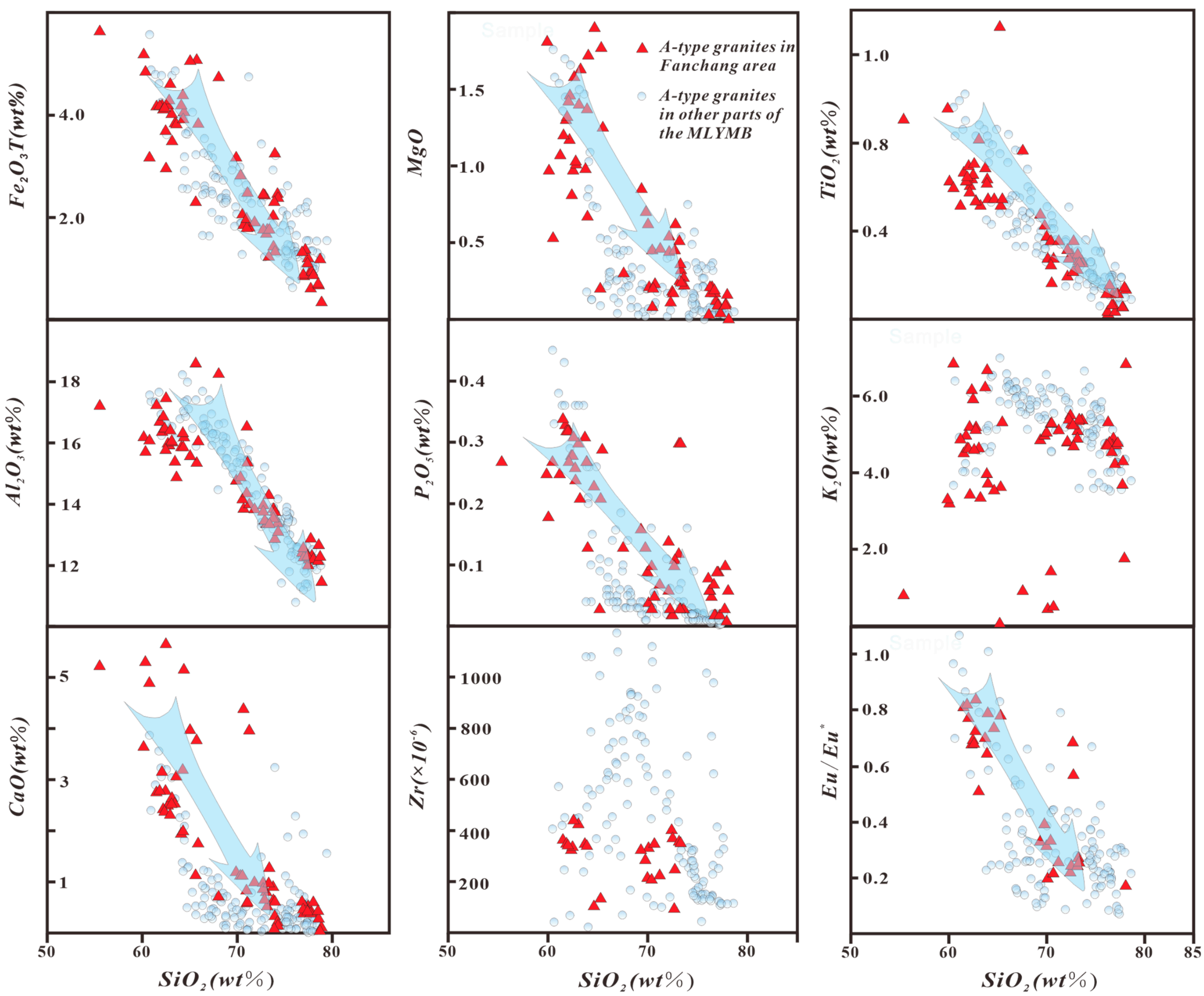

Figure 6. Harker diagrams of intrusive rocks in the FVB and other areas in the MLYMB.

The Zr-Zr/Y covariant diagram (Figure 7) can further identify the controlling role of orthopyroxene during the fractional crystallization or partial melting process. It can crystallize as separate cumulate phases during the crystallization process or remain as residual phases during the partial melting process [152].

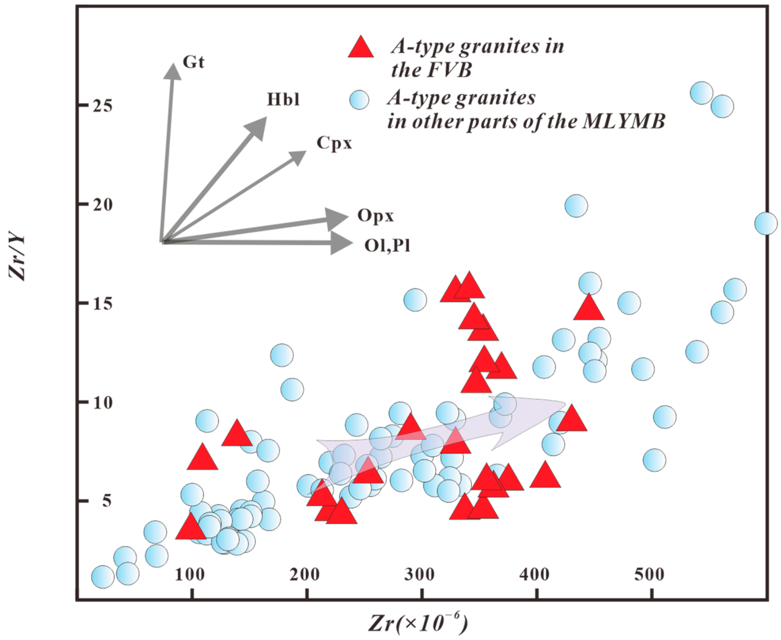

Figure 7. Zr/Y vs. Zr diagrams of A-type granite rocks in the FVB and other areas in the MLYMB (after [152]). Gt—garnet; Hbl—hornblende; Cpx—clinopyroxene; Opx—orthopyroxene; Ol—olivine; Pl—plagioclase.

The logarithmic diagrams of Ba-Sr and Rb-Sr (Figure 8) can reflect the fractional crystallization of K-feldspar, plagioclase, and other rock-forming minerals during the evolution of granitoid magmas [153]. The A-type granites in the FVB and in other areas of the MLYMB show trends suggesting fractionation of K-feldspar, plagioclase, and biotite.

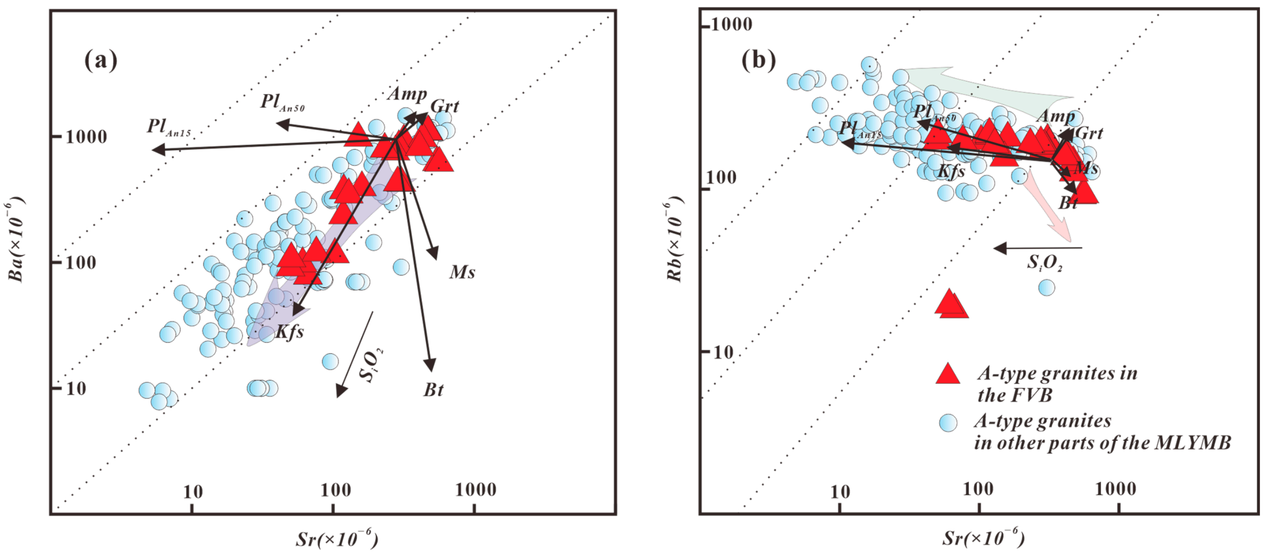

Figure 8. (**a**) Ba vs. Sr diagram and (**b**) Rb vs. Sr diagram of intrusive rocks in the FVB and A-type granites in other parts of the MLYMB (after [153]). Pl_{An50}: plagioclase (An = 50); plagioclase (An = 15); Kfs: K-feldspar; Bt: biotite; Ms: muscovite; Grt: garnet; Amp: amphibole.

In summary, we consider that the magmatic evolution of the A-type granites in the FVB and other areas in the MLYMB are mainly controlled by fractional crystallization, with orthopyroxene, plagioclase, K-feldspar, and biotite as the main crystallization phases.

4. Magmatic Source Characteristics of A-Type Granites in the FVB

According to ε_{Nd}(t)–(^{S7}Sr/^{86}Sr)$_i$ (Figure 9), the variation trend of Sr-Nd isotopes in the source area of the A-type granites in the FVB indicates that the source area is a mixture of three possible sources: the lithospheric mantle, late Archean Paleoproterozoic lower crust, and Neoproterozoic upper crust. The mantle endmember can be considered to consist of a somewhat enriched mantle, similar in composition to the basalts of the Kedoushan Formation (129.5 ± 3.3 Ma) [90,134,138]. The lower crustal endmember suggests late Archean or Paleoproterozoic crustal materials in the MLYMB, perhaps represented by the Kongling Group [154–157]. In addition, the Sr-Nd isotopes also show an obvious trend towards the Neoproterozoic crust in the Yangtze block [85,86]. However, this trend is mainly seen for A-type granites in other parts of the MLYMB, while the A-type granites in the FVB are dominated by the older lower crustal component in addition to the enriched mantle.

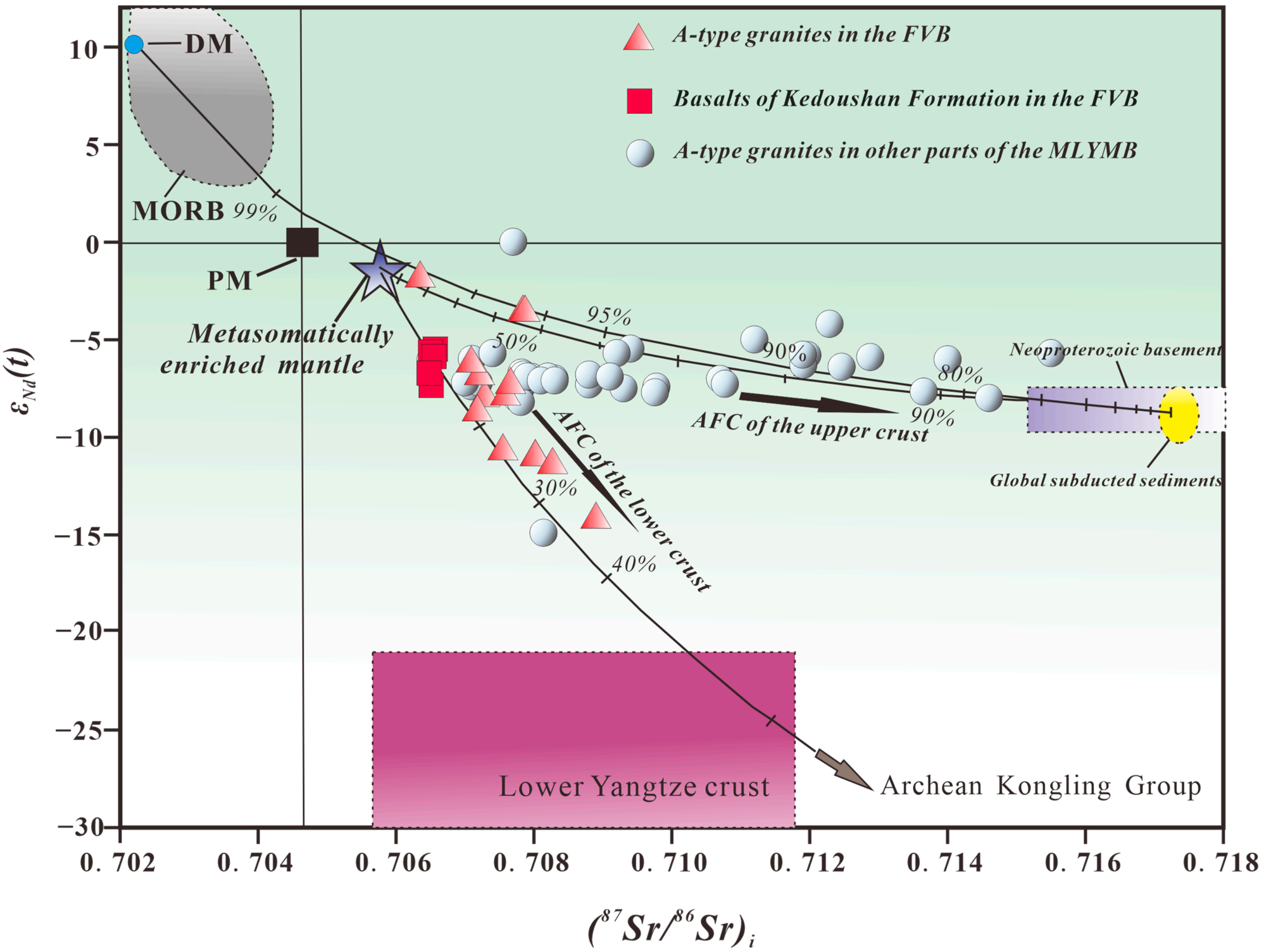

Figure 9. Diagram of initial ε_{Nd}(t) vs. initial (^{S7}Sr/^{86}Sr)$_i$ of A-type granites in the MLYMB. Data sources (see Supplement Table S3): Ocean basalt and primitive mantle [158]; metasomatically enriched mantle [138]; global subducted sediments [159]; Neoproterozoic basement [160]; Lower Yangtze crust [161]; A-type granites of the FVB [86,89]; A-type granites of the MLYMB [91,93,94,96,100,101,108,110].

The initial $\varepsilon_{Hf}(t)$ in zircon from A-type granites in the FVB dominantly falls between –4 and 10 (Figure 10), indicative of a Neoproterozoic crustal source. Therefore, some scholars believed that the Archean ancient material did not contribute to the magmatic source [85,134]. This is, however, at odds with the Nd isotope data from A-type granites in the FVB above, which indicated an Archean or Paleoproterozoic crustal source for these granites (Figure 9). In addition, the inherited zircons in the late Mesozoic magmatic rocks in the FVB and other parts of the MYLMB have multi-stage age ranges, also reflecting the involvement of Archaean–Paleoproterozoic and Neoproterozoic crustal materials [154–156,162].

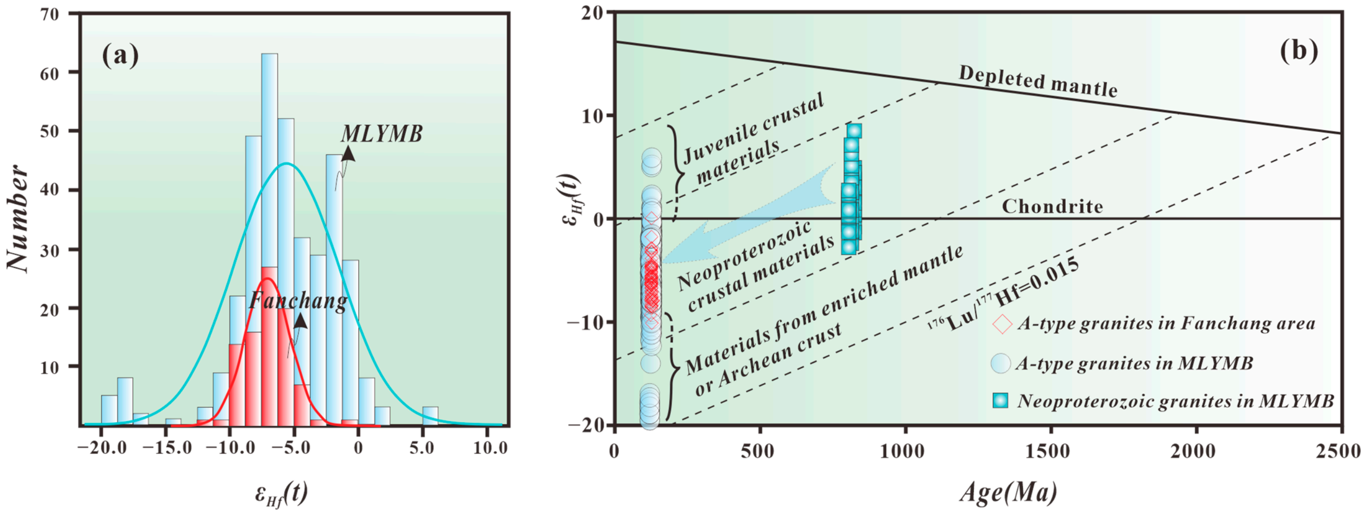

Figure 10. Diagram of initial $\varepsilon_{Hf}(t)$ vs. age of A-type granites in the MLYMB: (**a**) Histograms of $\varepsilon_{Hf}(t)$; (**b**) Diagram of $\varepsilon_{Hf}(t)$ vs. age. Data sources (see Supplement Table S4): A-type granites of the FVB [85,88]; A-type granites of the MLYMB [92–94,96,100,112].

Thus, when it comes to the apparent discrepancy between the indications of crustal components (Archean–Paleoproterozoic versus Neoproterozoic) from zircon Hf and whole rock Nd-Sr isotope data in the FVB, this may be simply an effect of too little Hf isotope data from the FVB granites, failing to capture the whole range of Hf isotope compositions, in combination with the fact that the Hf and Nd-Sr data have not been obtained from the same samples and therefore not directly comparable.

Compared to the FVB, the initial zircon $\varepsilon_{Hf}(t)$ of A-type granites in other areas of the MLYMB ranges from –20 to +6 (Figure 10 and Supplement Table S4). The low range of –20—-10 can be considered the result of the involvement of the enriched mantle or Archaean–Paleoproterozoic crust in the magmatic source [154], while the high range of 0–6 could be due to juvenile crust as a source [163], with the initial $\varepsilon_{Hf}(t)$ range of -10–0 corresponding to Neoproterozoic crustal materials. Combing with $\varepsilon_{Nd}(t)$–$(^{S7}Sr/^{86}Sr)_i$ (Figure 9), it can be concluded that the magmatic source area of A-type granites in other parts of the MLYMB included enriched mantle and Neoproterozoic crustal materials; perhaps Archean–Paleoproterozoic crust and juvenile crust are also involved.

To sum up, we believe that there are several sources of A-type granites in the FVB, with the enriched mantle, Archean–Paleoproterozoic lower crust, and Neoproterozoic upper crust involved. Compared with other areas in the MLYMB, the participation of ancient lower crust materials in the source area of A-type granites in the FVB may be higher.

5. Ore-Controlling Characteristics and Typical Deposits

Skarn-type and hydrothermal-type iron and zinc deposits are the main ore types closely related to the A-type granites in the FVB, and there is more of a gradual shift between them. They are mainly hosted in interlayer faults or other fractures in carbonate rocks as well as in contact zones with granites. The difference between them lies in whether there are obvious skarn minerals [113].

Gravity and magnetic anomaly features show that there are granite massifs below these mining areas; combined with the outcrops, these anomalies are likely to be A-type granites [77,113]. In addition, taking the Taochong and Suishan deposits as examples, granite can be seen in the deep part of the drillings at the edge of these mining areas (Figure 3d–f, Figure 11b and Figure 13). In terms of mineralization time, the Re-Os model age of pyrite in the Xiaoyangchong skarn stage indicates that its metallogenetic age is about 125.7 Ma [89], which is clearly located in the same age region as the A-type granites in the FVB.

The skarn-type ore bodies are always restricted to the contact zone between magmatic rocks and carbonate rocks or occur within faults in the granite massif. The hydrothermal deposits are mainly hosted within fracture zones in granite massifs or carbonate strata. The characteristic gangue minerals include calcite, diopside, and quartz, and the ore minerals are mainly specularite, hematite, magnetite, and sphalerite (Figure 3) [77,81,113,164].

The deposit and ore characteristics of the main typical deposits in the FVB are as follows.

5.1. Taochong Iron Ore Deposit

(1) Geological characteristics

The main structure of the mining area is a fan-shaped anticline with an axis trending northeast. The deposit is located in the northwest limb of the anticline (Figure 1). The ore body is controlled by the faults between the upper and lower limbs of a recumbent fold. There are diorite porphyrite, microcrystalline diorite, and syenite porphyry veins interspersed in the deposit, and the alteration mainly consists of skarn alteration, epidotization, and carbonation. The ore body occurs near the contact zone between skarn and limestone, and it is sickle-like or lamellar in profile (Figure 11) [80,113].

(2) Ore mineral characteristics

The natural types of ore are as follows: (1) iron ore in the outer skarn zone and (2) iron ore in the inner skarn belt. The content of pseudohematite and specularite is higher in the outer skarn zone than in the inner skarn belt, while the content of magnetite is relatively lower. The gangue minerals in the outer skarn zone are mainly calcite and quartz, while in the inner skarn belt, they are mainly garnet, followed by pyroxene, calcite, and quartz [77].

5.2. Xiaoyangchong Zinc-Iron Ore

(1) Geological characteristics

The deposit is located in the southeastern limb of an anticline, and early Permian limestone and pre-mineralization diorite porphyrite are the main host rocks (Figure 12). The diorite porphyrite is shaped like an irregular tube that branches toward the surface but is connected at depth. The surrounding limestone is altered to marble or skarn [77,113].

(2) Ore mineral characteristics

The natural types of ore are as follows: (1) massive zinc-iron ore; (2) disseminated magnetite; (3) iron-bearing breccia; and (4) massive limonite. The first has a dense and massive structure, while the latter three have disseminated, vein-like and brecciated, and massive structures, respectively.

Ore minerals are mainly sphalerite, magnetite, and hematite, with a small amount of specularite, limonite, pyrite, chalcopyrite, and gold. Gangue minerals include garnet, tremolite, epidote, wollastonite, quartz, and opal.

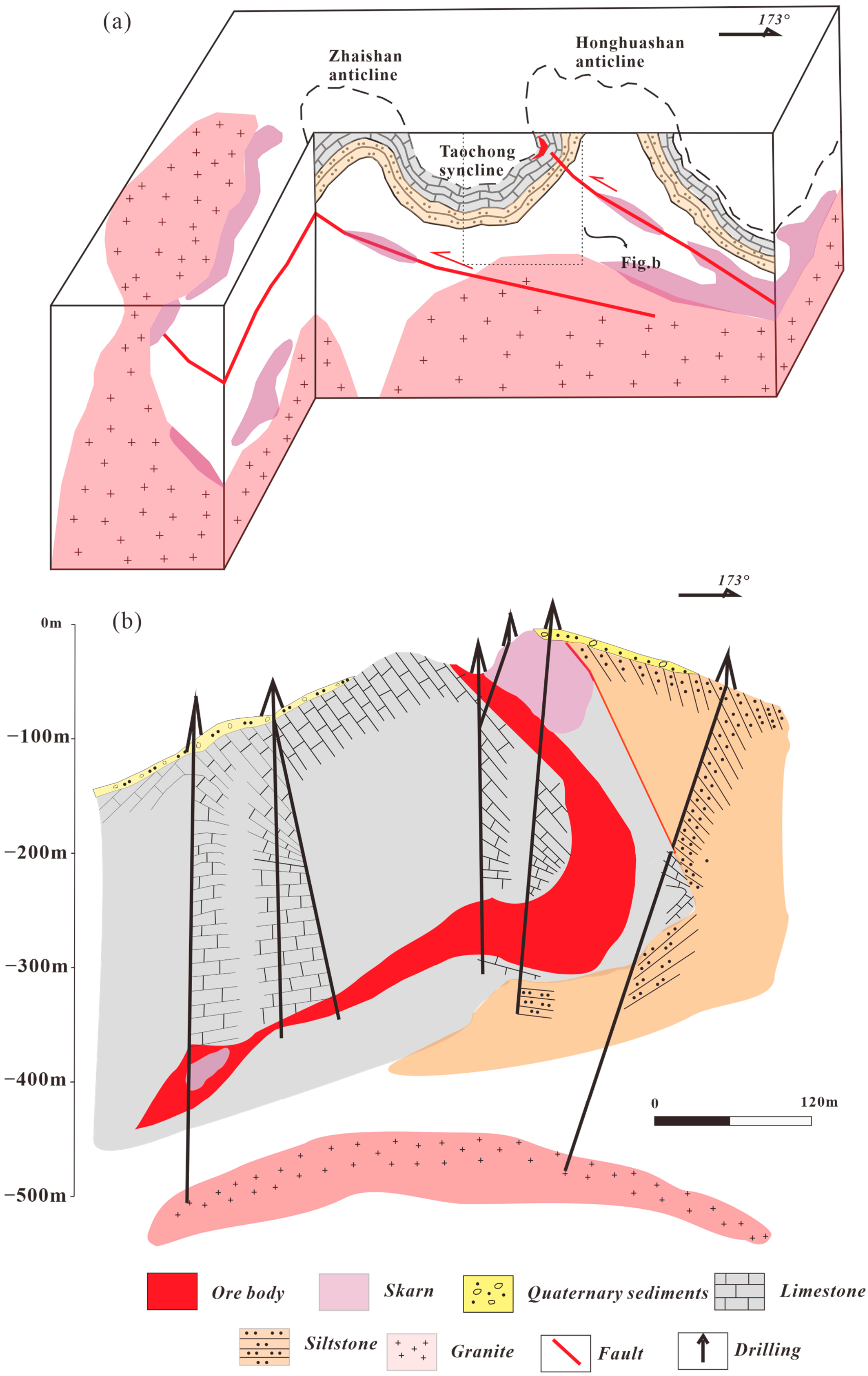

Figure 11. (**a**) Three-dimensional metallogenic model map (modified from [165]); (**b**) profile of the Taochong iron mine in the FVB (modified from [164]).

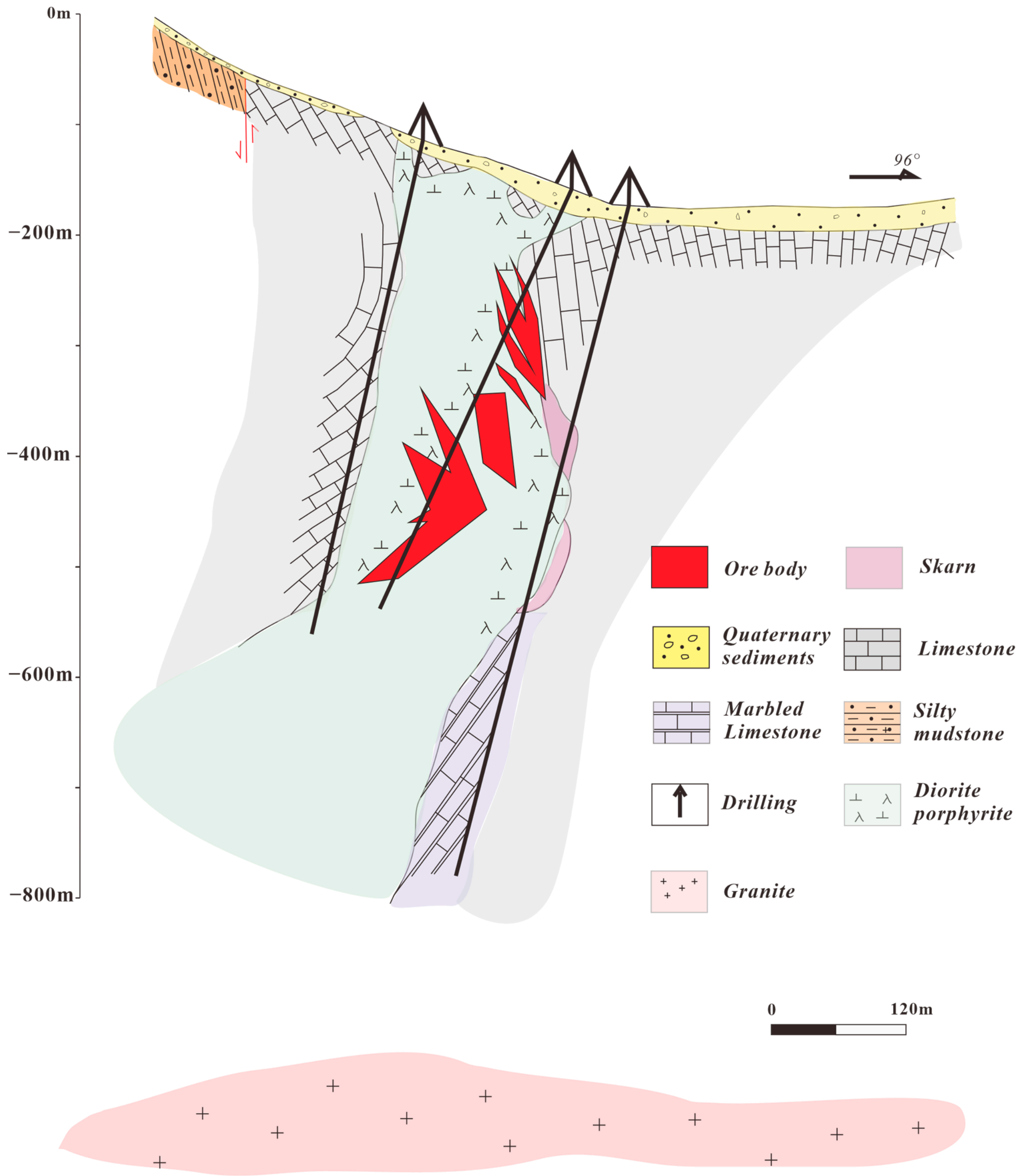

Figure 12. Geological profile of the Xiaoyangchong zinc–iron deposit in the FVB (modified from [77,113]).

5.3. Suishan Zinc Ore Deposit

(1) Geological characteristics

The deposit is hosted in the southeast limb of the Fanchang compound syncline, with the limestone of the upper member of the Lower Triassic Nanlinghu Formation being exposed in the area (Figure 1). The ore bodies are mainly lens-like (Figure 13) [113].

Skarnization and marmarization are closely related to zinc mineralization, with dolomitization, chloritization, and silicification processes also being involved. Skarn formation is the main alteration phenomenon in the area, and pyroxene and garnet skarns often have strong zinc mineralization, forming rich ore.

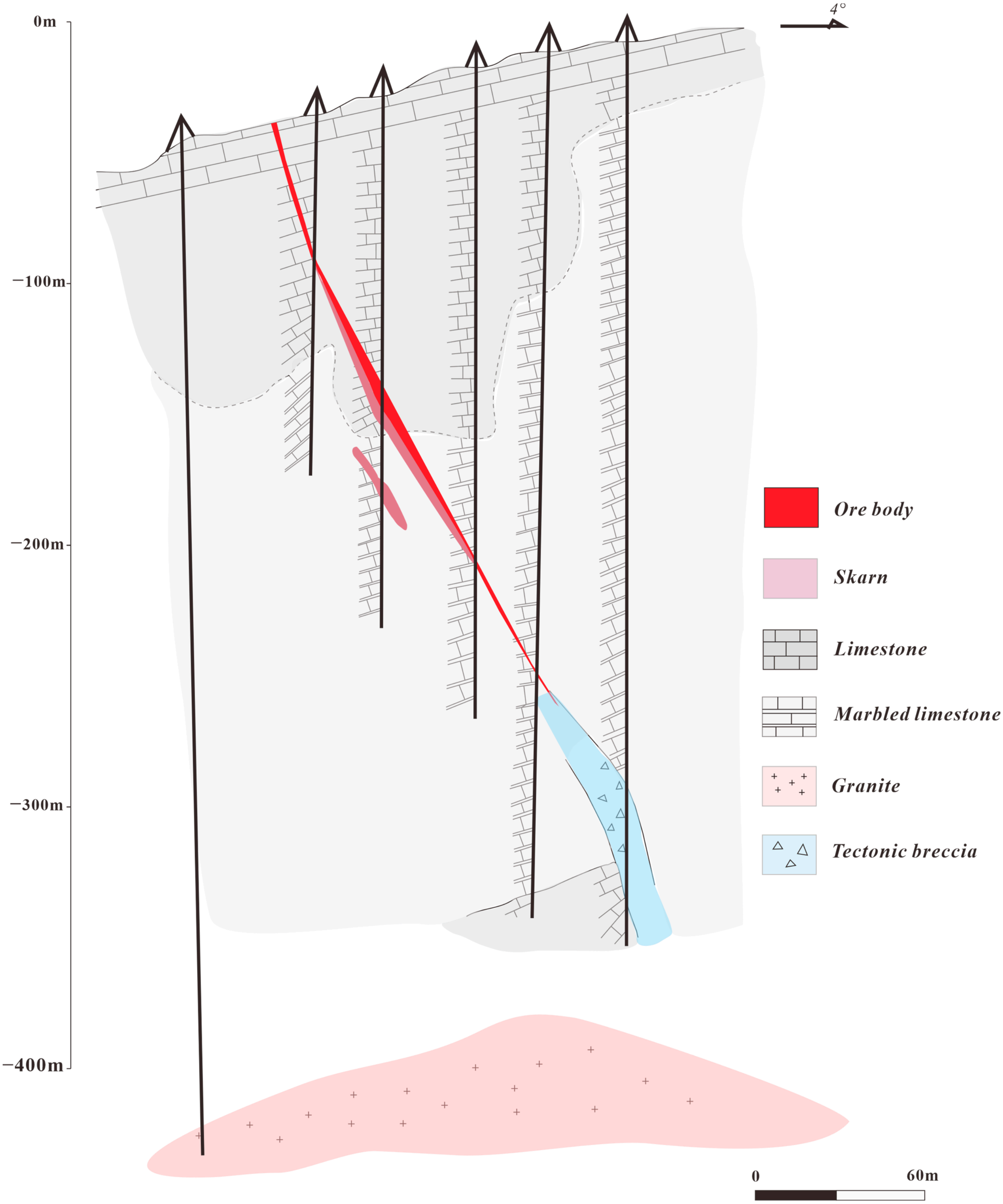

Figure 13. Geological profile of the Suishan zinc deposit in FVB (modified from [166]).

(2) Ore mineral characteristics

The natural types of ore are as follows: (1) massive sphalerite; (2) zinc-bearing skarn; and (3) zinc-bearing marble. The ore has massive, disseminated, banded, and brecciated structures.

Ore mineral composition: mainly sphalerite, pyrite, and cobaltite, followed by chalcopyrite, galena, specularite, and chalcocite, and with secondary minerals including limonite, siderite, and lead oxide. Gangue minerals are mainly pyroxene, garnet, and actinolite, followed by calcite, quartz, tourmaline, and epidote.

6. Metallogenesis

6.1. Genesis of Mineral Deposits

The ore minerals in the zinc–iron deposits in the FVB are mainly of hydrothermal origin [113] (Figure 14). Taking the Xiaoyangchong zinc–iron deposit as an example, the electron probe analysis shows that the magnetite in the zinc–iron deposit principally formed during the post-magmatic hydrothermal stage [89], and the main genetic types are the contact metasomatic-type and the skarn-type.

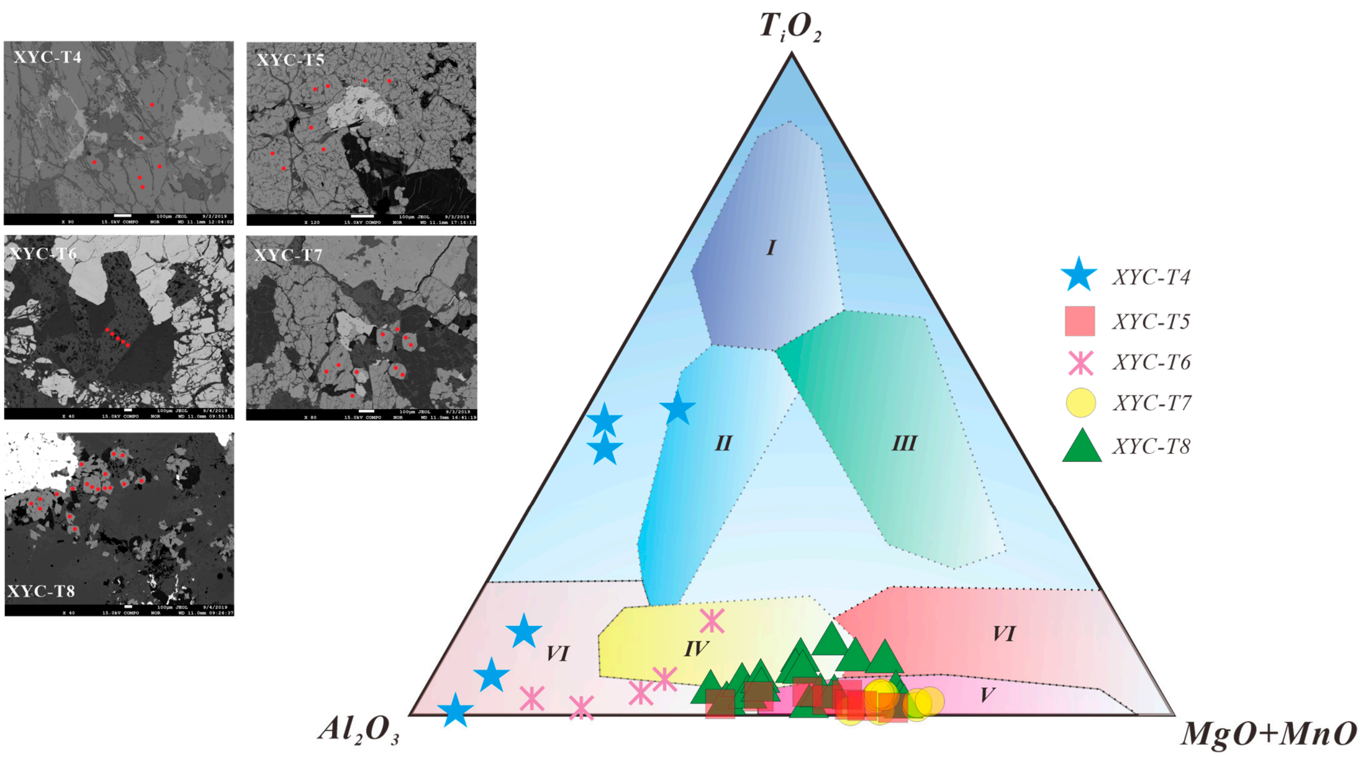

Figure 14. Genetic classification diagram of magnetite of the Xiaoyangchong deposit in the FVB (on the basis of [167]) (modified from [81]). Data sources (see Supplement Table S5): I—accessory mineral type; II—magma-type; III—volcanic-type; IV—contact metasomatic-type. V—skarn-type; VI—sedimentary metamorphic-type.

The studies on fluid inclusions and S isotopes of metal sulfides show that during the evolution process of skarn fluid to quartz–sulfide-bearing hydrothermal fluid, in addition to the mixing of magmatic water and meteoric water [80], there is also the presence of brine (hot brine formed by deep circulation of meteoric water or sealed hot brine), probably in association with the Triassic gypsum–salt formation (such as Triassic gypsum solution breccia, gravelly dolomite, etc.) (Figure 15) [81].

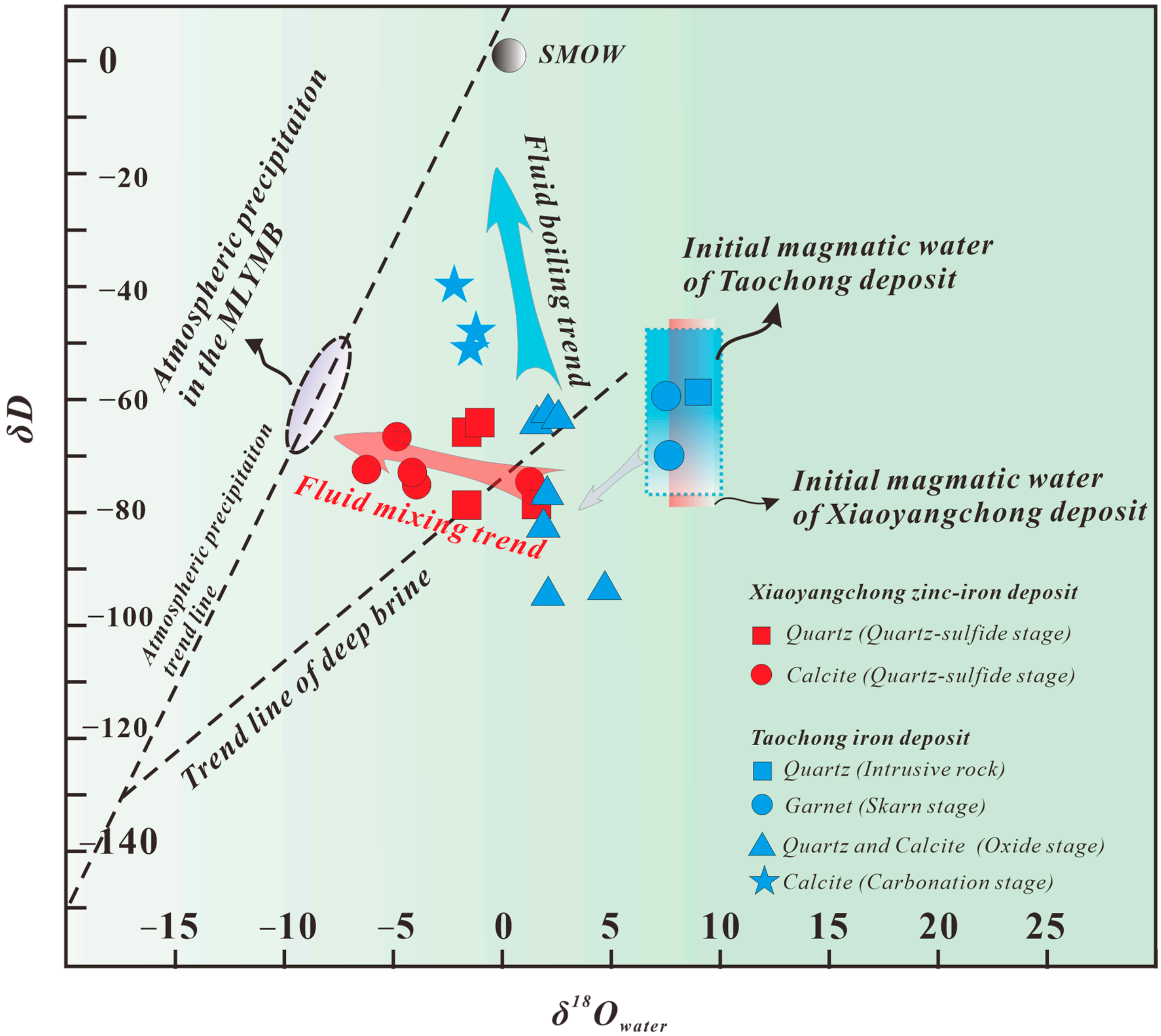

Figure 15. $\delta^{18}O$ water vs. δD plot of the isotopic composition of fluid inclusions in the typical deposits of the FVB. Data sources (see Supplement Table S6): Data of the Xiaoyanghcong and Taochong deposits are from [80,81]; range of Mesozoic meteoric water in the MLYMB is from [168,169]; fluid boiling trend is from [170].

The range of sulfur isotopic compositions of metal sulfides in skarn and hydrothermal deposits related to A-type granites in the FVB is relatively narrow ($\delta^{34}S$ = 5.8‰–19.2‰) (Figure 16); only metal sulfides are found in the ore rocks, no sulfate minerals, so the $\delta^{34}S$ of these metal sulfides should approximately represent the sulfur isotope composition of the hydrothermal system [171]. Possible sulfur sources of these deposits related to A-type granites include magmatic rocks (0.09‰–7.87‰, with an average value of 3.50‰), sedimentary clastic rocks (−16.7‰–−31.1‰, with an average value of −24.0‰), Triassic gypsum–salt strata (25.3‰–34.4‰, with an average value of 30‰) (Figure 16) [117,169]. Therefore, we consider that the sulfur in the skarn and hydrothermal deposits comes from two sources: A-type granite magma and gypsum–salt strata.

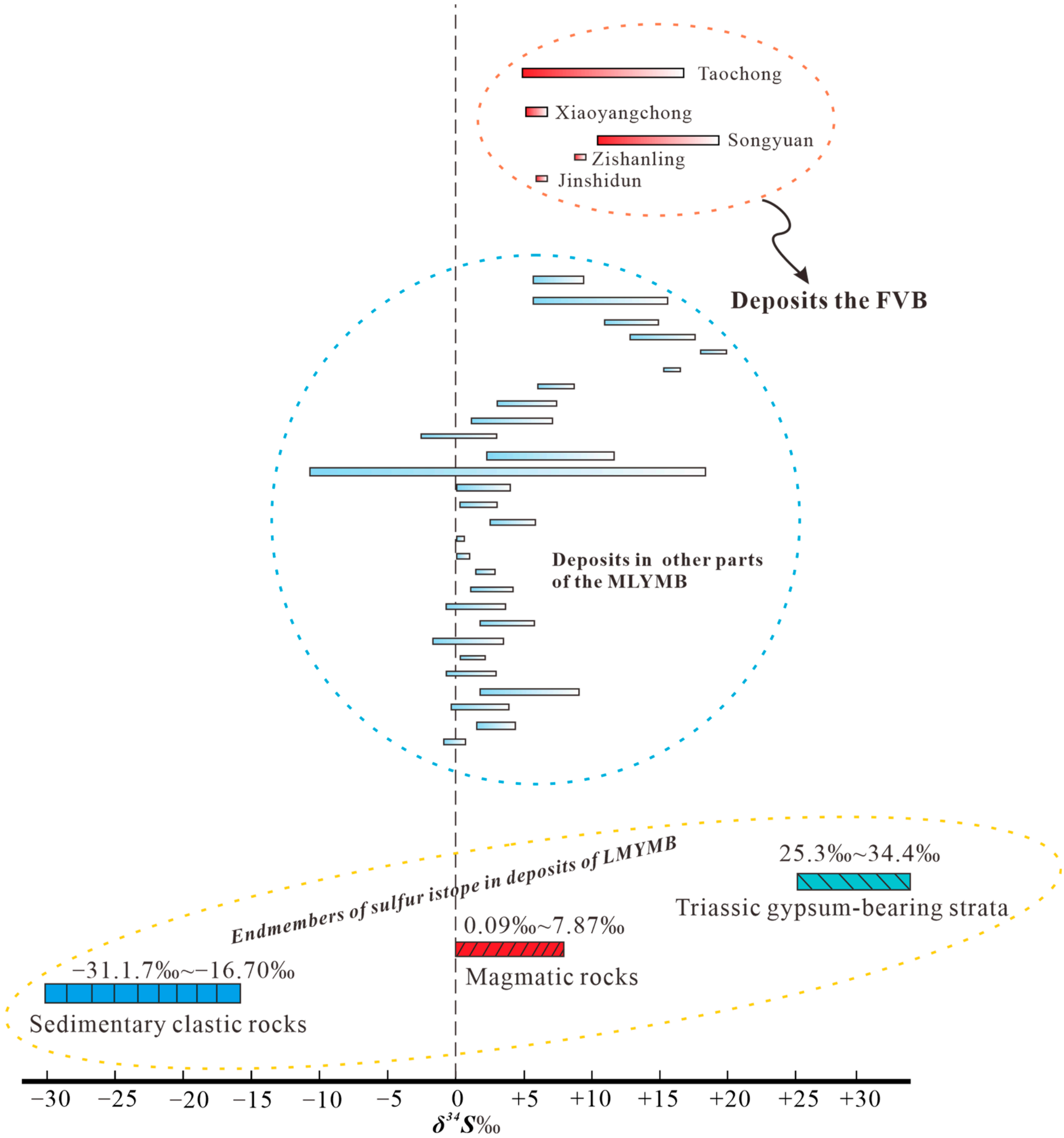

Figure 16. $\delta^{34}S$ ranges of metal sulfides from some typical skarn deposits in the FVB (see Supplement Table S7) and other Yanshanian deposits with endmembers of sulfur isotopes in the MLYMB (after [117]).

6.2. Metallogenic Potential

Pijajno [21] considered that metal precipitation depends on the oxygen fugacity of intrusive rocks in the order Sn–W–Mo–Cu-Mo–Cu-Au, with increasing oxygen fugacity, as well as on the iron content of intrusive rocks in the order Mo–Sn–W–Cu-Mo–Cu-Au, with increasing iron content. Blevin [20] suggested that four factors could determine the metallogenic potential of granitoids and related rocks: (1) the oxidation state; (2) compositional character (including alkalinity, petrogenic type, SiO_2 content, K_2O content, etc.); (3) degree of compositional evolution (e.g., Rb/Sr and K/Rb); and (4) the presence of fractionation. Zhao et al. [62] simplified the criteria to determine the mineralization potential of granitoids and believed that the types of granitoids (diorite, monzodiorite, monzonite, alkaline granite, etc.) reflected the comprehensive characteristics of the above four parameters [20], except for the oxidation state. Therefore, the combination of oxygen fugacity and rock type can ideally characterize the mineralization potential of granitoids [62].

As shown in Figure 17, Au and Cu (Au, Fe) correspond to the oxidized alkaline ore-forming system related to diorite and monzodiorite. Cu, Mo, W, Pb, and Ag correspond to the relatively reduced and peraluminous ore-forming system related to granodiorite (monzonite). Cu, Au, Mo, Fe, and Zn are related to the oxidized and peraluminous ore-forming system related to tonalite and monzonite. Sn, W, Be, Mo, F, and Zn correspond to a strongly reduced and peraluminous greisen metallogenic system related to granite or alkaline granite. Zn, Mo, F, W, and Ag tend to be formed in oxidized and peralkaline systems [62]. This is very consistent with the known metallogenic regularity of granite [172,173].

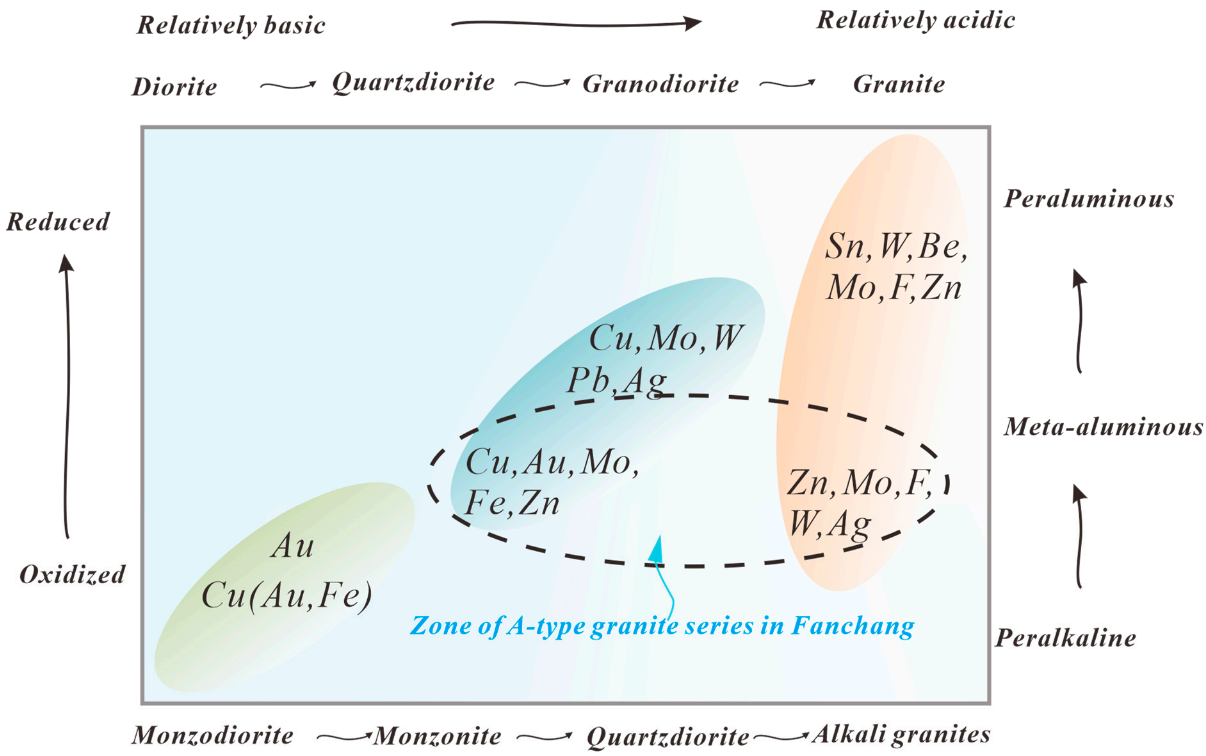

Figure 17. Schematic diagram of associations between mineralization and the chemistry of intrusions plus redox conditions [21,62].

Our previous studies have shown that for the A-type granites in the FVB, both the magmatic rocks and post-mineralization hydrothermal fluids are relatively oxidized [81,89]; the rock types are mainly K-feldspar granite, granite, and monzonite; and they essentially belong to the metaluminous intrusive types [81,89,174]. It can be seen from Figure 17 that besides Fe and Zn, the A-type granites in the FVB have prospecting potential for Cu, Au, Ag, Mo, etc. [172,173].

In other areas of the MLYMB, the mineralization related to A-type granites consists of Fe, U, Mo, and Au, etc. (Table 2) [77,92,114,164,175–179]. The A-type granites in the FVB are mostly identical to those in other parts of the MLYMB in terms of magmatic evolution characteristics (Figures 5–8), characteristics of major and trace elements [70,86,89], crystallization ages (Figure 3f), and magmatic source (Figures 9 and 10). The dominant metals in the ores related to the A-type granites in the FVB are mainly Zn and Fe, which seem to be different from other parts of the MLYMB (Table 2). However, from the perspective of metallogenic types and mineral compositions (Table 2), skarn and hydrothermal deposits are dominant, and sphalerite and magnetite are common in all these deposits. This indicates that the A-type granites in the FVB also potentially contain U, Mo, Au, and other metals.

Table 2. Summary of deposits related to A-type granites in the MLYMB.

No.	Location	Related Intrusive Rock Type	Deposit	Ore Type	Amount	Grade	Type of Ore	Alteration	Ore Minerals	Metallogenic Age			Metallogenic Type	References
										Mineral	Method	Age		
1	Fanchang	Banshiling, biotite quartz monzonite	Zishanling	Cu	No data	0.35%	Copper-bearing limonite ore and copper-bearing marble ore	Marbleization, skarnization, silicification, and chloritization	Chalcopyrite, bornite, and limonite	-	-	-	Hydrothermal-type	[113]
2	Fanchang	Binjiang, granitic porphyry	Taochong	Fe, Zn	34.71 Mt	44.29%	Skarn-type iron ore	Skarnization, breccification, marblelization, and silicification	Magnetite, hematite, and specularite	-	-	-	Layered skarn-type	[164]
3	Fanchang	Suishan, granite	Suishan	Zn	7331 t	10%	Massive zinc ore, zinc-bearing skarn ore, zinc-bearing marble ore	Skarnization, dolomitization, carbonation, chloritization, silicification, etc.	Mainly sphalerite, pyrite, and cobaltite	-	-	-	Skarn-type	[77]
4	Fanchang	Suishan, granite	Songyuan	S(Fe)	No data	28.35%	Pyrite ore	Garnet skarnization, carbonation, and silicification	Pyrite and specularite	-	-	-	Skarn-type	[77]
5	Fanchang	Xiaoyangchong, granodiorite	Xiaoyangchong	Zn (Fe)	Zn: 91,962 t; Fe: 2898 t	Zn: 6.7%; Fe: 37.97%	Massive zinc-iron ore, disseminated magnetite ore	Marbleization and skarnization	Sphalerite, magnetite, and hematite	Pyrite	Re-Os	125.7 Ma	Skarn-type	[77]
6	Chizhou	Huayuangong, Syenogranite	Liwan	Cu	40,000 t	0.62%	Copper-bearing pyrite, copper-bearing sulfur skarn, lead-zinc skarn	Marbleization and skarnization	Chalcopyrite, bornite, sphalerite, pyrite, and molybdenite	-	-	-	Skarn-type	[92]
7	Chizhou	Guilinzheng, granitic porphyry	Guilinzheng	Mo (W)	0.15 Mt	0.13%	Disseminated ore and banded ore	Silicification, sericitization, skarnization, and serpentinization	Molybdenite, sphalerite, molybdenum-rich scheelite, magnetite, and galena	-	-	-	Skarn-type	[114,179]
8	Anqing-Zongyang	Dalongshan, quartz syenite	Dalongshan	U	Small deposit	0.81%	Sandstone type ore and quartz syenite type ore	Hydromica, albitization, hematite, carbonation, silicification, pyritization, and chloritization	Pitchblende, microcrys-talline quartz, hematite, and pyrite	Pitchblende	U-Pb isochron method	130.0 Ma and 111.7 Ma	Hydrothermal-type	[178]
9	Anqing-Zongyang	Huangmeijian, quartz syenite	Dingjiashan	U	No data	0.1~0.2%	Sandstone type ore and quartz syenite type ore	Silicification, carbonation, chloritization, discoloration, pyritization, brass mineralization, and kaolinization	Pitchblende and uranium	Pitchblende	U-Pb isochron method	108.7 Ma	Hydrothermal-type	[176]

Table 2. *Cont.*

No.	Location	Related Intrusive Rock Type	Deposit	Ore Type	Amount	Grade	Type of Ore	Alteration	Ore Minerals	Metallogenic Age			Metallogenic Type	References
										Mineral	Method	Age		
10	Anqing-Zongyang	Huangmeijian, quartz syenite	Xucun	U	No data	0.28%	Felsic sandstone type and quartz syenite type	Silicitization, pyritization, carbonatization, greenization, and hydromicatization	Pitchblende and uranium	Single mineral zircon in pitchblende	U-Pb	108 ± 1.5 Ma and 71.3 ± 1.0 Ma	Hydrothermal-type	[116]
11	Anqing-Zongyang	Huangmeijian, quartz syenite	Makou	Fe	0.08 Mt	No data	Reticulated and massive magnetite ore	Potassic mineralization	Magnetite, apatite, pyrite, and sphalerite	Phlogopite	^{40}Ar-^{39}Ar	127.3 ± 0.8 Ma	Hydrothermal-type	[175]

6.3. Metallogenetic Mechanism

Most scholars consider that many A-type granites contain an abnormally high F content [1,3], and F is positively correlated with Fe, Zn, Nb, Zr, and Ga. These ore-forming elements can form stable complexes with fluorine [14]. In an oxidizing environment, Fe in a magmatic hydrothermal fluid mainly migrates in the form of a Fe^{3+}–F^{-} complex, and after entering a relatively reducing environment, the Fe^{3+} in the ore-forming fluid changes to Fe^{2+}, and the Fe^{3+}–F^{-} complex decompounds, resulting in the precipitation of a large amount of iron to form magnetite or pyrrhotite [180,181]. At high temperatures, zinc also forms a complex with F (such as ZnF_2) [182,183]. The above findings may explain the metallogenic mechanism of zinc and iron deposits formed by A-type granite magmatism in the FVB.

6.4. Preliminary Analysis of the Metallogenetic Potential of Key Metals

The chemical analysis results of iron and zinc ores from typical deposits in the FVB, both of skarn-type and hydrothermal-type ores, show their additional utilization potential as sources of Cd, Ga, and Se (Table 3) [77].

Table 3. Key metals associated with important deposits in the FVB [77].

Name of Mine	Exploration Stage	Ore Type	Associated Key Metal and Grade
Xiaoyangchong zinc-iron mine	Mining	Massive sphalerite and magnetite ores	Cd: 100–900 ppm
Suishan zinc mine	Mineral prospecting	Sphalerite ore and pyrite ore	Cd: 1111 ppm Se: 25–60 ppm
Shunfengshan iron mine	Detailed mineral prospecting	Magnetite ore	Ga: 21 ppm
Fuchengdun copper mine	Mineral prospecting	Chalcopyrite ore	Cd: 100 ppm

The metallic element cadmium has a very low abundance in the crust (0.2 ppm, [153]). Cadmium is mainly produced from lead–zinc mines, which account for 90% of the total cadmium resources. It has been generally believed that cadmium is mainly enriched in sphalerite by replacing Zn [184,185].

In this new round of comprehensive evaluations of metal resources in the FVB, it was found that the utilization potential of rare, scattered elements in zinc ores was great (Table 3), especially for cadmium. Taking the Xiaoyangchong zinc–iron deposit as an example, the Cd content of the massive sphalerite ore in the Xiaoyangchong mine reached an economic level for industrial production, with the content of Cd in massive magnetite ore also being relatively high. The content of Cd in sphalerite ore in the Suishan zinc deposit was also high, at 1111 ppm and 379 ppm, respectively, in two samples of sphalerite ore [77].

Ga can be enriched in metal sulfides instead of Fe, Zn, and Al, such as chalcopyrite, sphalerite, and bornite [186–188]. In the magnetite ore of the Shunfengshan iron mine, the content of Ga reaches 21 ppm. In addition, the anionic sulfur in sphalerite can be replaced by selenium to form selenium-rich sphalerite ore. The content of Se in sphalerite ore and pyrite ore in the Suishan zinc mine is high (25–60 ppm), reaching the economic levels of selenium.

7. Regional Petrogenetic and Metallogenetic Model

The crystallization temperatures of intrusive rocks in the FVB show a roughly rising trend (802 °C–931 °C) (Figure 18) [89], indicating that the high temperature conditions required for the formation of A-type granites were present during the extensional process [1–3,5]. This extension may have been caused by the roll-back movement of the Paleo-Pacific plate, resulting in upwelling of the asthenosphere [189–192]. As mentioned above, the A-type granites in the FVB are similar to coeval intrusions in the

MLYMB when it comes to the magma source, with a mixture of enriched mantle and crust [71,72,84,86,136,137,141,143] components. It can be suggested that asthenospheric upwelling led to the partial melting of the enriched subcontinental mantle [5,8]. Then, the enriched magma migrated upward and underwent assimilation and contamination from the lower crust to form intermediate magma [1,3,7]. During the continued upward migration of intermediate magma, assimilation and contamination with the upper crustal materials occurred [16,17], and plagioclase and other minerals crystallized as cumulate phases. In addition, fluorine-containing minerals in the crust entered the magma system [14], in which F^- could replace OH^-, forming skarn and hydrothermal ore deposits, as fluorine formed complexes with metals enriched in the A-type magma, which were concentrated into ore-forming hydrothermal solutions (Figure 18) [9,30].

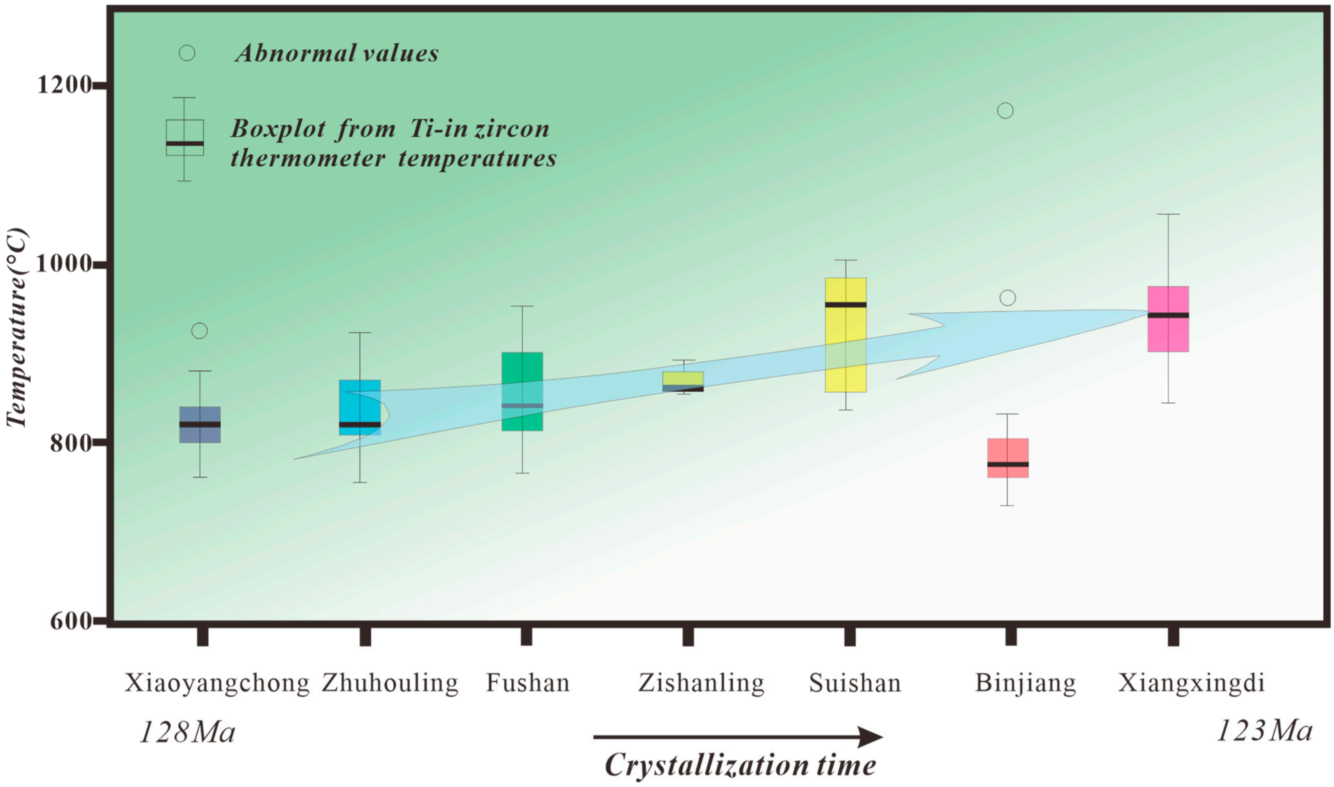

Figure 18. Crystallization temperature vs. crystallization time of A-type granites in the FVB (modified from [89]).

The A-type granite suite in the FVB mainly intruded into the dominating Triassic carbonate strata, forming skarn-type deposits in the contact zone between the granites and the carbonate strata or yielding hydrothermal-type mineralization along fault systems after the magmatic period. The ore-forming magmatic–hydrothermal fluid of the skarn deposits in the FVB was affected by mixing with gypsum salt brine and meteoric waters [89]. The gypsum salt layer is rich in $CaSO_4$, $MgSO_4$, and Cl^-, which is conducive to the extraction, migration, and transportation of iron, zinc, and other metal elements (Figure 19) [193,194].

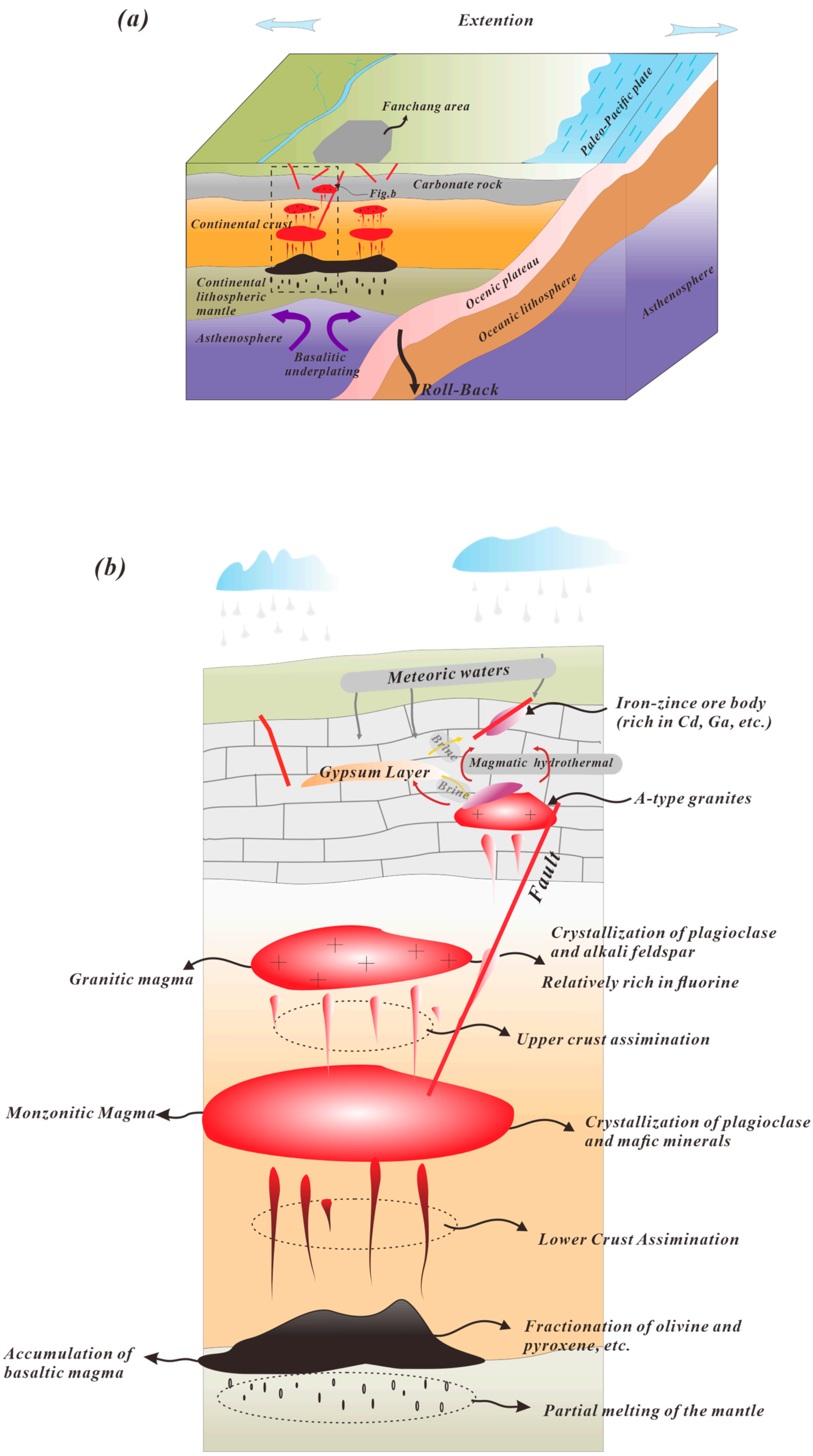

Figure 19. (**a**). Regional geotectonic model for the Triassic A-type granitic magmatism in the FVB and the MLYMB. (**b**). A more detailed petrogenetic and metallogenetic model for A-type magmatism and related ore formation in the FVB.

8. Conclusions

The A-type granites in the FVB are mainly similar to those in the other parts of the MLYMB in terms of magmatic evolution characteristics, with fractionation caused by the crystallization and separation of orthopyroxene, plagioclase, K-feldspar, and biotite. The magmatic source of A-type granites in the FVB is mixed and includes the enriched mantle, lower crust, and upper crust materials as components, perhaps with relatively stronger participation of Archaean–Paleoproterozoic crustal materials than that of other regions in the MLYMB. The main ore types of A-type granites in the FVB are skarn-type and hydrothermal-type ores, with the ore-forming fluid being a mixture of magmatic hydrothermal fluid, meteoric waters, and deep brine related to the gypsum–salt layer. The sulfur of metal sulfides may be a mixture of magmatically derived sulfur and sulfur originating from the Triassic gypsum-bearing layers. The iron and zinc ores in the FVB may be of interest also for the recovery of Cd, Ga, Se, and other minor elements contained within the ores. Furthermore, it is concluded that the FVB potentially harbors Cu, Au, Ag, Mo, etc., in addition to the already known metals in the area.

Supplementary Materials: The following supporting information can be downloaded at: https://www.mdpi.com/article/10.3390/min13040571/s1, Table S1: Major and trace elements of A-type granites in the MLYMB; Table S2: Crystallization ages of A-type granites in the MLYMB; Table S3: Sr and Nd isotope composition of A-type granites in the MLYMB; Table S4: Zircon Hf isotopic data of A-type granites in the MLYMB; Table S5: Electron probe analysis results of magnetites in Xiaoyangchong deposit, the FVB; Table S6: Stable H and O isotope compositions in fluid inclusions in minerals of typical skarn deposits in the FVB; Table S7: Sulfur isotopes of metal sulfides in typical deposits in the FVB.

Author Contributions: Conceptualization, S.Z. and X.Y.; methodology, X.Y.; software, S.Z.; validation, X.Y.; formal analysis, X.Y. and L.L.; resources, S.Z., X.Y. and L.L.; data curation, S.Z.; writing—original draft preparation, S.Z.; review and editing, S.Z., X.Y. and L.L.; visualization, S.Z.; supervision, X.Y. and L.L.; project administration, S.Z.; funding acquisition, X.Y. All authors have read and agreed to the published version of the manuscript.

Funding: This work was financially supported by the Natural Science Foundation of China (No. 42030801 and 42230801).

Acknowledgments: Special thanks to Johansson from the Department of Geosciences, Swedish Museum of Natural History, who put forward a lot of constructive and detailed comments for this paper. Thanks to Du Jianguo and Huang Yonghai, as well as Zhang Shu, Bai Ruyu, and Zhang Zanzan from the Anhui Geological Survey Institute, China, for providing some important geological data. Comments and suggestions from three anonymous reviewers helped improve this manuscript, and we also express our sincere thanks to them.

Conflicts of Interest: The authors declare no conflict of interest.

References

1. Collins, W.J.; Beams, S.D.; White, A.J.R.; Chappell, B.W. Nature and origin of A-type granites with particular reference to southeastern Australia. *Contrib. Mineral. Petrol.* **1982**, *80*, 189–200. [CrossRef]
2. Clemens, J.D.; Holloway, J.R.; White, A.J.R. Origin of an A-type granite; Experimental constraints. *Am. Mineral.* **1986**, *7*, 317–324.
3. Whalen, J.B.; Currie, K.L.; Chappell, B.W. A-type granites: Geochemical characteristics, discrimination and petrogenesis. *Contrib. Miner. Petr.* **1987**, *95*, 407–419. [CrossRef]
4. Fang, D.J.; Cai, H.L. The nature, genesis and metallogenic relationship of A-type granite in Zhejiang province. *Bull. Mineral. Petrol. Geochem.* **1987**, *6*, 234–235, (In Chinese with English abstract).
5. Eby, G.N.; Woolley, A.R.; Ross, M. The A-type granitoids: A review of their occurrence and chemical characteristics and speculations on their petrogenesis. *Lithos* **1990**, *26*, 115–134. [CrossRef]
6. Gu, L.X. Geological features, petrogenesis and metlallogeny of A-type granites. *Geol. Sci. Technol. Inf.* **1990**, *9*, 25–31, (In Chinese with English abstract).
7. Creaser, R.A.; Price, R.C.; Wormald, R.J. A-type granites revisited: Assessment of a residual-source model. *Geology* **1991**, *19*, 163–166. [CrossRef]
8. Eby, G.N. Chemical subdivision of the A-type granitoids: Petrogenetic and tectonic implications. *Geology* **1992**, *20*, 641–644. [CrossRef]

9. Patino Douce, A.E.P. Generation of metaluminous A-type granites by low-pressure melting of calc-alkaline granitoids. *Geology* **1997**, *25*, 743. [CrossRef]
10. King, P.L.; White, A.J.R.; Chappell, B.W.; Allen, C.M. Characterization and origin of aluminous A-type Granites from the Lachlan Fold Belt, Southeastern Australia. *J. Petrol.* **1997**, *38*, 371–391. [CrossRef]
11. Wu, S.P.; Wang, M.Y.; Qi, K.J. Present situation of researches on A-type granites: A review. *Acta Petrol. Mineral.* **2007**, *26*, 57–66, (In Chinese with English abstract).
12. Wong, J.; Sun, M.; Xing, G.F.; Li, X.H.; Zhao, G.C.; Wong, K.; Yuan, C.; Xia, X.P.; Li, L.M.; Wu, F.Y. Geochemical and zircon U-Pb and Hf isotopic study of the Baijuhuajian metaluminous A-type granite: Extension at 125–100 Ma and its tectonic significance for South China. *Lithos* **2009**, *112*, 289–305. [CrossRef]
13. Zhang, Q.; Ran, H.; Li, C.D. The criteria and discrimination for A-type granites: A reply to the question put forward by Wang Yang and some other persons for A-type granite: What is the essence? *Acta Petrol. Mineral.* **2012**, *31*, 621–626, (In Chinese with English abstract).
14. Akgul, B. Geochemical associations between fluorite mineralization and A-type shoshonitic magmatism in the Keban-Elazig area, East Anatolia, Turkey. *J. Afr. Earth Sci.* **2015**, *111*, 222–230. [CrossRef]
15. Zhao, J.L.; Qiu, J.S.; Liu, L.; Wang, R.Q. Geochronological, geochemical and Nd-Hf isotopic constraints on the petrogenesis of Late Cretaceous A-type granites from the southeastern coast of Fujian Province, South China. *J. Asian Earth Sci.* **2015**, *105*, 338–359. [CrossRef]
16. Johansson, Å. A Tentative Model for the Origin of A-Type Granitoids. *Minerals* **2023**, *13*, 236. [CrossRef]
17. Johansson, Å.; Waight, T.; Andersen, T.; Simonsen, S.L. Geochemistry and petrogenesis of Mesoproterozoic A-type granitoids from the Danish island of Bornholm, southern Fennoscandia. *Lithos* **2016**, *244*, 94–108. [CrossRef]
18. Lehmann, B. Metallogeny of tin; magmatic differentiation versus geochemical heritage. *Econ. Geol.* **1982**, *77*, 50–59. [CrossRef]
19. King, P.L.; Chappell, B.W.; Allen, C.M.; White, A.J.R. Are A-type granites the high temperature felsic granites? Evidence from fractionated granites of the Wangrah Suite. *Aust. J. Earth Sci.* **2001**, *48*, 501–514. [CrossRef]
20. Blevin, P.L. Redox and Compositional Parameters for Interpreting the Granitoid Metallogeny of Eastern Australia: Implications for Gold-rich Ore Systems. *Resour. Geol.* **2004**, *54*, 241–252. [CrossRef]
21. Pirajno, F. *Hydrothermal Process and Mineral System*; Springer: Berlin/Heidelberg, Germany, 2008; pp. 1–1238.
22. Pirajno, F.; Mao, J.W.; Zhang, Z.C.; Zhang, Z.H.; Chai, F.M. The association of mafic-ultramafic intrusions and A-type magmatism in the Tian Shan and Altay orogens, NW China: Implications for geodynamic evolution and potential for the discovery of new ore deposits. *J. Asian Earth Sci.* **2008**, *32*, 165–183. [CrossRef]
23. Yang, Y.Z.; Wang, Y.; Ye, R.S.; Li, S.Q.; He, J.F.; Siebel, W.; Chen, F.K. Petrology and geochemistry of Early Cretaceous A-type granitoids and late Mesozoic mafic dikes and their relationship to adakitic intrusions in the lower Yangtze River belt, Southeast China. *Int. Geol. Rev.* **2016**, *59*, 62–79. [CrossRef]
24. Zheng, W.; Mao, J.W.; Zhao, H.J.; Zhao, C.S.; Yu, X.F. Two Late Cretaceous A-type granites related to the Yingwuling W-Sn polymetallic mineralization in Guangdong province, South China: Implications for petrogenesis, geodynamic setting, and mineralization. *Lithos* **2017**, *274–275*, 106–122. [CrossRef]
25. Xin, W.; Sun, F.Y.; Li, L.; Yan, J.M.; Zhang, Y.T.; Wang, Y.C.; Shen, T.S.; Yang, Y.J. The Wulonggou metaluminous A2-type granites in the Eastern Kunlun Orogenic Belt, NW China: Rejuvenation of subduction-related felsic crust and implications for post-collision extension. *Lithos* **2018**, *312–313*, 108–127. [CrossRef]
26. Jia, R.Y.; Wang, G.C.; Geng, L.; Pang, Z.S.; Jia, H.X.; Zhang, Z.H.; Chen, H.; Liu, Z. Petrogenesis of the Early Cretaceous Tiantangshan A-Type Granite, Cathaysia Block, SE China: Implication for the Tin Mineralization. *Minerals* **2019**, *9*, 257. [CrossRef]
27. Kaur, P.; Chaudhri, N.; Eliyas, N. Chlorine-rich amphibole and biotite in the A-type granites, Rajasthan, NW India: Potential indicators of subsolidus fluid-rock interaction and metallogeny. *Geol. J.* **2019**, *54*, 614–630. [CrossRef]
28. Mao, C.; Lü, X.; Chen, C. Geochemical Characteristics of A-Type Granite near the Hongyan Cu-Polymetallic Deposit in the Eastern Hegenshan-Heihe Suture Zone, NE China: Implications for Petrogenesis, Mineralization and Tectonic Setting. *Minerals* **2019**, *9*, 309. [CrossRef]
29. Vasyukova, O.; Williams, J.A. Partial melting, fractional crystallisation, liquid immiscibility and hydrothermal mobilization—A 'recipe' for the formation of economic A-type granite-hosted HFSE deposits. *Lithos* **2020**, *356–357*, 105300. [CrossRef]
30. Vonopartis, L.C.; Kinnaird, J.A.; Nex, P.A.M.; Robb, L.J. African A-Type granites: A geochemical review on metallogenic potential. *Lithos* **2021**, *396–397*, 106229. [CrossRef]
31. Chappell, B.W.; White, A. Two contrasting granite types. *Pac. Geol.* **1974**, *8*, 173–174.
32. Maaloe, S.; Wyllie, P.J. Water content of a granite magma deduced from the sequence of crystallization determined experimentally with water undersaturated conditions. *Contrib. Mineral. Petrol.* **1975**, *52*, 175–191. [CrossRef]
33. Loiselle, M.C.; Wones, D.R. Characteristics and origin of anorogenic granites. *Geol. Soc. Am. Abst. Prog.* **1979**, *11*, 468.
34. Barbarin, B. A review of the relationships between granitoid types, their origins and their geodynamic environment. *Lithos* **1999**, *46*, 605–626. [CrossRef]
35. Chappell, B.W.; White, A.J.R. Two contrasting granite types: 25 years later. *Aust. J. Earth Sci.* **2001**, *48*, 489–499. [CrossRef]
36. Frost, B.R.; Barnes, C.G.; Collins, W.J.; Arculus, R.J.; Ellis, D.J.; Frost, C.D. A geochemical classification for granitic rocks. *J. Petrol.* **2001**, *42*, 2033–2048. [CrossRef]

37. Wu, F.Y.; Li, X.H.; Yang, J.H.; Zheng, Y.F. Discussions on petrogenesis of granites. *Acta Petrol. Sin.* **2007**, *23*, 1217–1238, (In Chinese with English abstract).
38. White, A.J.R.; Chappell, B.W. Ultrametamorphism and granitoid genesis. *Tectonophysics* **1977**, *43*, 7–22. [CrossRef]
39. Nardi, L.; Bonin, B. Post-orogenic and non-orogenic alkaline granite associations: The Sibro intrusive suite, southern Brazil: A case study. *Chem. Geol.* **1991**, *92*, 197–211. [CrossRef]
40. Whalen, J.B.; Hildebrand, R.S. Trace element discrimination of arc, slab failure, and A-type granitic rocks. *Lithos* **2019**, *348–349*, 105179. [CrossRef]
41. Turner, S.P.; Foden, J.D.; Morrison, R.S. Derivation of some A-type magmas by fractionation of basaltic magma: An example from the Padthaway Ridge, South Australia. *Lithos* **1992**, *28*, 151–179. [CrossRef]
42. Wu, F.Y.; Sun, D.Y.; Li, H.M.; Jahn, B.M.; Wilde, S. A-type granites in northeastern China: Age and geochemical constraints on their petrogenesis. *Chem. Geol.* **2002**, *187*, 143–173. [CrossRef]
43. Martin, R. A-type granites of crustal origin ultimately result from open-system fenitization-type reactions in an extensional environment. *Lithos* **2006**, *91*, 125–136. [CrossRef]
44. Yang, J.H.; Wu, F.Y.; Chung, S.L.; Wilde, S.A.; Chu, M.F. A hybrid origin for the Qianshan A-type granite, northeast China: Geochemical and Sr–Nd–Hf isotopic evidence. *Lithos* **2006**, *89*, 89–106. [CrossRef]
45. Bonin, B. A-type granites and related rocks: Evolution of a concept, problems and prospects. *Lithos* **2007**, *97*, 1–29. [CrossRef]
46. Li, H.; Ling, M.X.; Li, C.Y.; Zhang, H.; Ding, X.; Yang, X.Y.; Fan, W.M.; Li, Y.L.; Sun, W.D. A-type granite belts of two chemical subgroups in central eastern China: Indication of ridge subduction. *Lithos* **2012**, *150*, 26–36. [CrossRef]
47. Liu, P.; Mao, J.W.; Santosh, M.; Bao, Z.A.; Zeng, X.J.; Jia, L.H. Geochronology and petrogenesis of the Early Cretaceous A-type granite from the Feie'shan W-Sn deposit in the eastern Guangdong Province, SE China: Implications for W-Sn mineralization and geodynamic setting. *Lithos* **2018**, *300–301*, 330–347. [CrossRef]
48. Li, Y.J.; Wei, J.H.; Tan, J.; Fu, L.B.; Li, H.; Ke, K.J. Albian Cenomanian A-type granite-related Ag-Pb-Zn veins in the central Yidun Terrane, SW China: Constraints from the Xiasai deposit. *Miner. Depos.* **2020**, *55*, 1047–1070. [CrossRef]
49. Hong, D.W.; Wang, S.G.; Han, B.F.; Jin, M.Y. Classification of tectonic environment of alkaline granites and their identification criteria. *Sci. China Ser. B* **1995**, *4*, 418–426, (In Chinese with English abstract).
50. Liu, C.S.; Chen, X.M.; Chen, P.R.; Wang, R.C.; Hu, H. Subdivision, discrimination and genesis for A-type rock suite. *Geol. J. China Univ.* **2003**, *9*, 573–591, (In Chinese with English abstract).
51. Chen, D.L.; Liu, L.; Che, Z.C.; Luo, J.H.; Zhang, Y.X. Determination and preliminary study of Indosinian aluminous A-type granites in the Qimantag area, southeastern Xinjiang. *Geochimica* **2001**, *30*, 540–546, (In Chinese with English abstract).
52. Fu, J.M.; Ma, C.Q.; Xie, C.F.; Zhang, Y.M.; Peng, S.B. Geochemistry and tectonic setting of Xishan aluminous A-type granitic volcanic-intrusive complex Southern Hunan. *J. Earth Sci. Environ.* **2004**, *26*, 15–23, (In Chinese with English abstract).
53. Liu, C.S.; Chen, X.M.; Wang, R.C.; Zhang, W.L.; Hu, H. Isotopic dating and origin of complexly zoned micas for A-type Nankunshan aluminous granite. *Geol. Rev.* **2005**, *51*, 193–200+227, (In Chinese with English abstract).
54. Burnham, C.W.; Ohmoto, H. Late-stage processes of felsic magmatism. *Geol. Spec. Issue* **1980**, *8*, 1–11.
55. Ishihara, S. The granitoid series and mineralization. *Econ. Geol.* **1981**, *75*, 458–484.
56. Ishihara, S.; Izawa, E.; Shimazaki, H. Granitoid series and mineralization in the Circum-Pacific Phanerozoic granitic belts. *Resour. Geol.* **2010**, *48*, 219–224. [CrossRef]
57. Ishihara, S. Granitoid Series and REE-Y-Zr-Ta-Nb Mineralization. *Mater. Sci. Forum* **1991**, *70–72*, 527–536. [CrossRef]
58. Blevin, P.L.; Chappell, B.W. The role of magma sources, oxidation states and fractionation in determining the granite metallogeny of eastern Australia. *Earth Environ. Sci. Trans. R. Soc. Edinb.* **1992**, *83*, 305–316.
59. Thompson, J.F.H.; Sillitoe, R.H.; Baker, T.; Lang, J.R.; Mortensen, J.K. Intrusion-related gold deposits associated with tungsten-tin provinces. *Miner. Depos.* **1999**, *34*, 323–334. [CrossRef]
60. Huston, D.L.; Mernagh, T.P.; Hagemann, S.G.; Doublier, M.P.; Fiorentini, M.; Champion, D.C.; Jaques, A.L.; Czarnota, K.; Cayley, R.; Skirrow, R.; et al. Tectono-metallogenic systems-The place of mineral systems within tectonic evolution, with an emphasis on Australian examples. *Ore Geol. Rev.* **2016**, *76*, 168–210. [CrossRef]
61. Blevin, P.L.; Chappell, B.W.; Allen, C.M. Intrusive metallogenic provinces in eastern Australia based on granite source and composition. *Trans. R. Soc. Edinb. Earth Sci.* **1996**, *87*, 281–290.
62. Zhao, B.; Zhang, D.H.; Shi, C.L.; Zhang, R.Z. Rethinking of the metallogenic specialization and ore bearing potential of redox related granitoid. *Acta Petrol. Mineral.* **2014**, *33*, 955–964, (In Chinese with English abstract).
63. Huang, H.; Zhang, Z.C.; Santosh, M.; Zhang, D.Y. Geochronology, geochemistry and metallogenic implications of the Boziguo'er rare metal-bearing peralkaline granitic intrusion in South Tianshan, NW China. *Ore Geol. Rev.* **2014**, *61*, 157–174. [CrossRef]
64. Chen, X.C.; Zhao, C.H.; Zhu, J.J.; Wang, X.S.; Cui, T. He, Ar, and S isotopic constraints on the relationship between A-type granites and tin mineralization: A case study of tin deposits in the Tengchong-Lianghe tin belt, southwest China. *Ore Geol. Rev.* **2018**, *92*, 416–429. [CrossRef]
65. Liu, C.F.; Zhao, S.H.; Liu, W.C. The relationship between gold mineralization, high K calc-alkaline to alkaline volcanic rocks, and A-type granite: Formation of the Daxiyingzi gold deposit in northern North China Craton. *Ore Geol. Rev.* **2021**, *138*, 104383. [CrossRef]

66. Zhang, X.J.; Liu, W.H.; Lentz, D.R.; Wu, Z.H.; Wu, Y.H.; Zhang, X.P.; Yang, S.L. Tin enrichment in a highly fractionated A-type granite: Origin and mineralization potential of the Dayishan granite batholith in the Shi-Hang magmatic zone, South China. *Ore Geol. Rev.* **2022**, *140*, 104603. [CrossRef]
67. Chang, Y.F.; Liu, X.P.; Wu, Y.C. *The Copper-Ion Belt of the Lower and Middle Districts of the Yangtze River*; Geological Publishing House: Beijing, China, 1991; pp. 1–379.
68. Zhai, Y.S.; Yao, S.Z.; Lin, X.D. Metallogenic regularity of iron and copper deposits in the middle and lower valley of the Yangtze River. *Miner. Depos.* **1992**, *11*, 1–12, (In Chinese with English abstract).
69. Zhou, T.F.; Fan, Y.; Yuan, F. Advances on petrogenesis and metallogeny study of the mineralization belt of the middle and lower reaches of the Yangtze River area. *Acta Petrol. Sin.* **2008**, *24*, 1665–1678, (In Chinese with English abstract).
70. Xie, X.B.; Yang, M.; Cong, G.X. Study on A-type granitoids in the middle and lower reaches of the Yangtze River. *South. Met.* **2015**, 15–21, (In Chinese with English abstract).
71. Mao, J.W.; Zhou, T.F.; Xie, G.Q.; Yuan, F.; Duan, C. Metallogeny in Middle-Lower Yangtze River Ore Belt: Advances and problems remained. *Miner. Depos.* **2020**, *39*, 547–558, (In Chinese with English abstract).
72. Zhou, T.F.; Fan, Y.; Chen, J.; Xiao, X.; Zhang, S. Critical metal resources in the Middle-Lower Yangtze River Valley metallogenic belt. *Sci. China Press* **2020**, *65*, 3665–3677, (In Chinese with English abstract). [CrossRef]
73. Hua, R.M.; Fu, P.R.; Chen, W.L.; Liu, X.D.; Lu, J.J.; Lin, J.F.; Yao, J.M.; Qi, H.W.; Zhang, Z.S.; Gu, S.Y. Mesozoic and Cenozoic metallogenic systems related to granitoids in south China. *Sci. China Ser. D* **2003**, *33*, 335–343, (In Chinese with English abstract).
74. Wang, D.Z. The study of granitic rocks in south China: Looking back and forward. *Geol. J. China Univ.* **2004**, *10*, 305–314, (In Chinese with English abstract).
75. Xing, F.M.; Xu, X. Two A-type granite belts from Anhui. *Acta Petrol. Sin.* **1994**, *13*, 357–369, (In Chinese with English abstract).
76. Wang, Y.L.; Li, Z.Y.; Wang, Y. Analysis on the metallogenic characteristics of rich iron ore in Fanchang area. *Express Inf. Min. Ind* **2007**, 75–77, (In Chinese with English abstract).
77. Du, J.G.; Lu, S.M.; Wu, L.B. *Mineral Geology of China: Volume of Anhui Province*; Geological Publishing House: Beijing, China, 2020; pp. 1–541.
78. Wang, D.Z.; Zhao, G.T.; Qiu, J.S. The tectonic constraint on the Late Mesozonic A-type granitoids in eastern China. *Geol. J. Univ.* **1995**, *1*, 13–21, (In Chinese with English abstract).
79. Liu, L.S.; Chen, S.X. Geological characteristics and prospecting signs of Changlongshan iron deposit in Fanchang County, Anhui Province. *Mordenmining* **2010**, *26*, 64–67, (In Chinese with English abstract).
80. Cao, Y.; Du, Y.S.; Gao, F.P.; Hu, L.F.; Xin, F.P.; Pang, Z.S. Origin and evolution of hydrothermal fluids in the Taochong iron deposit, Middle-Lower Yangtze Valley, Eastern China: Evidence from microthermometric and stable isotope analyses of fluid inclusions. *Ore Geol. Rev.* **2012**, *48*, 225–238. [CrossRef]
81. Zhang, S.S.; Yang, X.Y.; Li, W.; Wang, K.Y.; Han, Z.S.; Yang, Y.L. Study of ore-forming fluid and ore-forming age of skarn-type iron ore in Fanchang area. *Acta Geol. Sin.* **2022**, *96*, 1297–1320, (In Chinese with English abstract).
82. Lou, Y.E. Characteristics and Petrogenesis of the Mesozoic Intrusive Rocks in Fanchang, Anhui Province. Ph.D. Thesis, China University of Geosciences (Beijing), Beijing, China, 2005; pp. 1–103, (In Chinese with English abstract).
83. Lou, Y.E.; Du, Y.S. Characteristics and zircon SHRIMP U-Pb ages of the Mesozoic intrusive rocks in Fanchang, Anhui province. *Ceochemica* **2006**, *35*, 359–366, (In Chinese with English abstract).
84. Wu, F.Y.; Ji, W.Q.; Sun, D.H.; Yang, Y.H.; Li, X.H. Zircon U-Pb geochronology and Hf isotopic compositions of the Mesozoic granites in southern Anhui Province, China. *Lithos* **2012**, *150*, 6–25. [CrossRef]
85. Yan, J.; Peng, G.; Liu, J.M.; Li, Q.Z.; Chen, Z.H.; Shi, L.; Liu, X.Q.; Jiang, Z.Z. Petrogenesis of granites from Fanchang district, the lower Yangtze region: Zircon geochrology and Hf-isotopes constrains. *Acta Petrol. Sin.* **2012**, *28*, 3209–3227, (In Chinese with English abstract).
86. Yan, J.; Liu, J.M.; Li, Q.Z.; Xing, G.F.; Liu, X.Q.; Xie, J.C.; Chu, X.Q.; Chen, Z.H. In situ zircon Hf-O isotopic analyses of late Mesozoic magmatic rocks in the Lower Yangtze River Belt, central eastern China: Implications for petrogenesis and geodynamic evolution. *Lithos* **2015**, *227*, 57–76. [CrossRef]
87. Mao, J.W.; Duan, C.; Liu, J.L.; Zhang, C. Metallogeny and corresponding mineral deposit model of the Cretaceous terrestrial volcanic-intrusive rocks-related polymetallic iron deposits in Middle-Lower Yangtze River Valley. *Acta Petrol. Sin.* **2012**, *28*, 1–14, (In Chinese with English abstract).
88. Pang, Z.S.; Gao, F.P.; Zhu, X.Q.; Dong, Q.; Lin, L.J. Petrogenesis and tectonic implications of the Fushan moyite in the Fanchang area, Anhui Province-Evidence from zircon U-Pb age, geochemistry and Hf isotopes. *Geol. Bull. China* **2017**, *36*, 402–417, (In Chinese with English abstract).
89. Zhang, S.S.; Yang, X.Y.; Wang, K.Y.; Han, C.S.; Yang, Y.L. Geochronological and geochemical constraints on the origin of the Mesozoic granitoids in the Fanchang volcanic basin, the Middle-Lower Yangtze Metallogenic Belt. *Solid Earth Sci.* **2021**, *6*, 178–204. [CrossRef]
90. Liu, C.; Yan, J.; Song, C.Z.; Li, Q.Z.; Peng, G.; Shi, L.; Liu, X.Q. Geochronology and geochemistry of the volcanic rocks from Fanchang basin in the middle-lower Yangtze River: Petrogenesis and geological significances. *Acta Petrol. Sin.* **2012**, *28*, 3228–3240, (In Chinese with English abstract).
91. Peng, G. Petrogenesis and Deep Processes of Late Mesozoic A-Type Granite in the Lower Yangtze Region. Master's Thesis, Hefei University of Technology, Hefei, China, 2012; pp. 1–83, (In Chinese with English abstract).

92. Duan, L.A.; Gu, H.L.; Yang, X.Y.; Yan, Z.Z.; Sun, W.D. Chronology and Hf isotopic study of igneous rocks in the Liwan Cu-polymetal deposit in Guichi along the Middle-Lower Yangtze River. *Acta Petrol. Sin.* **2015**, *31*, 1943–1961, (In Chinese with English abstract).
93. Yang, Y.Z. Geochemical Studies of Copper Related adakitic Rocks and the Magmatic Rocks of Post-Mineralization in the Middle-Lower Yangtze Belt. Ph.D. Thesis, University of Science and Technology of China, Beijing, China, 2015; pp. 1–219, (In Chinese with English abstract).
94. Gu, H.L. The Yanshanian Magmatism and Its Relations to the Cu (Mo)-Au Mineralization in Guichi District, Lower Yangtze River Metallogenic Belt. Ph.D. Thesis, University of Science and Technology of Chin, Hefei, China, 2017; pp. 1–212, (In Chinese with English abstract).
95. Jiang, X.Y.; Ling, M.X.; Wu, K.; Zhang, Z.K.; Sun, W.D.; Sui, Q.L.; Xia, X.P. Insights into the origin of coexisting A1- and A2-type granites: Implications from zircon Hf-O isotopes of the Huayuangong intrusion in the Lower Yangtze River Belt, eastern China. *Lithos* **2018**, *318–319*, 230–243. [CrossRef]
96. Yang, C.; Yan, J.; Wang, S.N.; Song, S.M.; Zhang, D.Y.; Liu, J.M. Petrogenesis of the late Mesozoic Bashan complex in the Lower Yangtze River Belt, eastern China: Implications for the definition and significance of A-type granite. *Lithos* **2021**, *392–393*, 106114. [CrossRef]
97. Cao, Y.; Du, Y.S.; Cai, C.L.; Qin, X.L.; Li, S.T.; Xiang, W.S. Mesozoic A-type Granitoids and xenoliths in the Lujiang-Zongyang area, Anhui province: Significance in post-collisional magmatic evolution. *Geol. J. China Univ.* **2008**, *14*, 565–576, (In Chinese with English abstract).
98. Fan, Y.; Zhou, T.F.; Yuan, F. LA-ICP-MS zircon U-Pb ages of the A-type granites in the Lu-zong (Lujiang-Zongyang) area and their geological significances. *Acta Petrol. Sin.* **2008**, *24*, 1715–1724, (In Chinese with English abstract).
99. Li, H.; Zhang, H.; Ling, M.X.; Wang, F.Y.; Ding, X.; Zhou, J.B.; Yang, X.Y.; Tu, X.L.; Sun, W.D. Geochemical and zircon U-Pb study of the Huangmeijian A-type granite: Implications for geological evolution of the Lower Yangtze River belt. *Int. Geol. Rev.* **2011**, *53*, 499–525. [CrossRef]
100. Wu, Q.; Niu, M.L.; Zhu, G.; Wang, T.; Fei, L.L. Zircon U-Pb age, petrogenesis of the Changgang A-type granites in the Lujiang segment of the Tan-Lu fault zone and their implication. *Acta Petrol. Sin.* **2016**, *32*, 1031–1048, (In Chinese with English abstract).
101. Du, X. Discussion on Genesis of A-Type Granite in Southern Luzong Basin. Master's Thesis, Hefei University of Technology, Hefei, China, 2018; pp. 1–75, (In Chinese with English abstract).
102. Zhang, J.K. Characteristics and Petrogenesis of the Dalongshan Granitoids in Anqing Area. Master's Thesis, China University of Geosciences (Beijing), Beijing, China, 2018; pp. 1–51, (In Chinese with English abstract).
103. Luo, X.W. Whole-Rock Element and Zircon U-Pb-Hf Isotope Study of Dalongshan and Huangmeijian Granitoids in the Middle-Lower Yangtze Region and Their Geological Significances. Master's Thesis, East China University of Technology, Nanchang, China, 2019; pp. 1–72, (In Chinese with English abstract).
104. Huang, Y.M. The Diagenesis of Fanchang Basin and Ore Mineralization of Taochong. Master's Thesis, Hefei University of Technology, Hefei, China, 2010; pp. 1–84, (In Chinese with English abstract).
105. Song, C.Z.; Jiang, Q.S.; Li, J.H.; Yan, J.; Shi, Y.H.; Han, Z.S.; Huang, W.P.; Yu, G. Relationship between structures and their controls to ores in the southern margin of Fanchang Basin in Anhui Province. *Acta Petrol. Sin.* **2012**, *28*, 3197–3208, (In Chinese with English abstract).
106. Yang, C.B.; Lu, J.H. Geological characteristics and genesis of Xiaozi mountain lead-zinc deposit in Fanchang county, Anhui Province. *Geol. Prospect.* **2018**, 194–195, (In Chinese with English abstract).
107. Zhou, T.F.; Fan, Y.; Yuan, F.; Chuan, C.Z.; Zhang, L.J.; Qian, C.C.; Lu, S.M.; David, R.C. Temporal-spatial framework of magmatic intrusions in Luzong volcanic basin in east China and their constrain to mineralizations. *Acta Petrol. Sin.* **2010**, *26*, 2694–2714, (In Chinese with English abstract).
108. Liu, Y.Y.; Ma, C.Q.; Lu, Z.Y.; Huang, W.P. Zircon U-Pb age, element and Sr-Nd-Hf isotope geochemistry of Late Mesozoic magmatism from the Guichi metallogenic district in the Middle and Lower Reaches of the Yangtze River Region. *Acta Petrol. Sin.* **2012**, *28*, 3287–3305, (In Chinese with English abstract).
109. Zhang, S.; Zhou, T.F.; Zhang, Z.Z.; Lu, B.; Shi, L.S.; Wang, J.; Wu, M. Geochronology of Huangmeijian composite pluton in Middle-lower Yangtze River Valley metallogenic belt, China: Implications on the petrogenesis and metallogeny. *J. Earth Sci. Environ.* **2022**, *44*, 220–242, (In Chinese with English abstract).
110. Cao, Y. Studies on Mesozoic A-Type Granitoids and Their Rock Xenoliths in Lujiang-Zongyang Area. Master's Thesis, China University of Geosciences (Beijing), Beijing, China, 2008; pp. 1–68, (In Chinese with English abstract).
111. Yang, C. The Yanshannian Intrusive Rocks and Their Relationship with Metallogenesis in the Chizhou Area, Lower Yangtze River Belt. Ph.D. Thesis, Hefei University of Technology, Hefei China, 2021; pp. 1–278, (In Chinese with English abstract).
112. Luo, X.W.; Wang, A.D.; Lai, D.R.; Li, Q.Z.; Wan, J.J.; Li, X.C. Zircon U-Pb Chronology and Hf Isotope of Dalongshan and Huangmeijian A-type Granites in Anhui Province. *Sci. Technol. Eng.* **2018**, *18*, 1–15, (In Chinese with English abstract).
113. Bureau of Geology and Mineral Resources, Anhui Province. *Regional Geological Survey Report: 1/50000 Hengshanqiao, Wuhu, Fanchang and Huangmu Duzhang*; Printing Factory of Surveying and Mapping Team of Bureau of Geology and Mineral Resources: Hefei, China, 1989; pp. 1–249, (In Chinese with English abstract).

114. Chen, X.F.; Zhou, T.F.; Zhang, D.Y.; Xiong, Z.Y.; Lu, Q.L.; Yuan, F.; Ren, Z.; Fan, Y. Geochronology, geochemistry and geological characteristics of the granite porphyry beneath Guilinzheng Mo deposit, Chizhou, southern Anhui. *Acta Petrol. Sin.* **2017**, *33*, 3200–3216, (In Chinese with English abstract).
115. Zhai, J.P.; Xu, G.P.; Zhang, B.T.; Hu, K. Comagmatic characteristics of the Luzong Volcanic Rocks and subalkaline quartz syenite rock-belt and their genesis. *Geol. Rev.* **1999**, *45*, 707–711, (In Chinese with English abstract).
116. Yang, B.; Liu, C.C.; Zhou, Q.; Zhang, Z.Z.; Xiao, J.G.; Cao, D.W. Geological characteristics, genesis and metallogenic model of Xuncun uranium deposit in the northern margin of Huangmeijian intrusive body, Anhui Province. *East China Geol.* **2021**, *42*, 318–329, (In Chinese with English abstract).
117. Zhou, T.F.; Yue, S.C.; Yuan, F.; Liu, X.D.; Zhao, Y. Isotopes of hydrogen, oxygen, sulfur and lead in two series of copper and gold deposits and their ore-forming fluid system in the Middle and Lower Reaches of the Yangtze River. *Sci. China Ser. D* **2000**, *30*, 122–128, (In Chinese with English abstract).
118. Chang, Y.F.; Zhou, T.F.; Fan, Y. Polygenetic compound mineralization and tectonic evolution: Study in the Middle-Lower Yangtze River Valley metallogenic belt. *Acta Petrol. Sin.* **2012**, *28*, 3067–3075, (In Chinese with English abstract).
119. Yang, X.Y.; Gu, H.L.; Yan, Z.Z.; Lu, Q.L.; Duan, L.; Deng, J.H.; Zhu, Y.S.; Wang, M.S.; Zhao, D.K. Metallogenic relationship between Yanshanian magmatic rocks and Cu-Au-Mo deposits in Guichi area of Anhui: Evidence from geological-geochemical-geophysical characteristics. *J. Earth Sci. Environ.* **2016**, *38*, 444–463, (In Chinese with English abstract).
120. Xu, X.C.; An, Y.H.; Xu, X.Y.; Fu, Z.Y. Ziron U-Pb ages and element geochemistry characteristics of magmatic rocks in Nanling-Xuancheng area of Anhui, China. *J. Earth Sci. Environ.* **2020**, *42*, 15–35, (In Chinese with English abstract).
121. Xing, F.M.; Xu, X. High-potassium calc-alkaline intrusive rocks in Tongling area, Anhui province. *Geochimica* **1996**, *25*, 29–38, (In Chinese with English abstract).
122. Du, Y.S.; Qin, X.L.; Li, X.J. Mesozoic mantle-derived magma underplating in Tongling, Anhui Province from megacrysts and Xenoliths. *Acta Petrol. Min.* **2004**, *23*, 109–116, (In Chinese with English abstract).
123. Du, Y.S.; Li, S.T.; Cao, Y.; Qin, X.L.; Lou, Y.E. UAFC-related origin of the late Jurassic to early Cretaceous intrusions in the Tongguanshan ore field, Tongling, Anhui province, east China. *Geoscience* **2007**, *21*, 71–77, (In Chinese with English abstract).
124. Xu, X.C.; Bai, R.Y.; Xie, Q.Q.; Lou, J.W.; Zhang, Z.Z.; Liu, Q.N.; Chen, L.W. Re-understanding of the geological and geochemical characteristics of the Mesozoic intrusive rocks from Tongling area of Anhui Province, and discussions on their genesis. *Acta Petrol. Sin.* **2012**, *28*, 3139–3169, (In Chinese with English abstract).
125. Jiang, S.Y.; Duan, D.F.; Xu, Y.M.; SAMAKE, B.; Li, Z.H. Geological characteristic and discrimination criteria of the ore related granitoids from the E'dong and Juirui districts in the Middle-Lower Yangtze Metallogenic Belt. *Acta Petrol. Sin.* **2019**, *35*, 3609–3628, (In Chinese with English abstract).
126. Mao, J.W.; Xie, G.Q.; Duan, C.; Pirajno, F.; Ishiyama, D.; Chen, Y.C. A tectono-genetic model for porphyry-skarn-strata bound Cu-Au-Mo-Fe and magnetite-apatite deposits along the Middle-Lower Yangtze River Valley, Eastern China (EI). *Ore Geol. Rev.* **2011**, *43*, 294–314. [CrossRef]
127. Yao, L.; Xie, G.Q.; Zhang, C.S.; Liu, J.L.; Yang, H.B.; Zheng, X.W.; Liu, X.F. Mineral characteristics of skarns in the Chengchao large-scale Fe deposit of southeastern Hubei Province and their geological significance. *Acta Petrol. Sin.* **2012**, *28*, 133–146, (In Chinese with English abstract).
128. Zhao, H.J.; Xie, G.Q.; Wei, K.T.; Ke, Y.F. Mineral compositions and fluid evolution of the Tonglushan skarn Cu-Fe deposit, SE Hubei, east-central China. *Int. Geol. Rev.* **2012**, *54*, 737–764. [CrossRef]
129. Xie, G.Q.; Mao, J.W.; Zhu, Q.Q.; Yao, L.; Li, Y.H.; Li, W.; Zhao, H.J. Geochemical constraints on Cu-Fe and Fe skarn deposits in the E'dong district, Middle-Lower Yangtze River metallogenic belt, China. *Ore Geol. Rev.* **2015**, *64*, 425–444. [CrossRef]
130. Ningwu Research Project's Writing Group. *Porphyrite Iron Ore in Ningwu Area*; Geological Publishing House: Beijing, China, 1978; pp. 69–78.
131. Zhang, Q.; Jian, P.; Liu, D.Y.; Wang, Y.L.; Qian, Q. Zircon SHRIMP dating of Ningwu volcanic rocks and its significance. *Sci. China Ser. D* **2003**, *33*, 309–314, (In Chinese with English abstract).
132. Liu, Z.; Yang, X.Y.; Liu, C.M.; Huang, D.Z.; Zhou, W.J.; Teng, X.; Liang, E.Y.; Dai, T.G. Genesis of Early Cretaceous porphyrite-type iron deposits and related sub-volcanic rocks in the Ningwu Volcanic Basin, Middle-Lower Yangtze Metallogenic Belt, Southeast China. *Int. Geol. Rev.* **2018**, *60*, 1507–1528. [CrossRef]
133. Geology and Mineral Resources Bureau of Anhui Province. *Regional Geology of Anhui Province*; Geological Publishing House: Beijing, China, 1987; pp. 1–723.
134. Liu, J.M.; Yan, J.; Chen, D.D.; Li, Q.Z.; Liu, X.Q.; Yao, H.Z.; Shi, L.; Chen, Z.H. Petrogenesis of the volcanic rocks in Fanchang basin, the Middle-Lower Yangtze River Belt: Zircon Hf-O isotopic constraints. *Acta Petrol. Sin.* **2016**, *32*, 289–302, (In Chinese with English abstract).
135. Yan, J.; Liu, H.Q.; Song, C.Z.; Xu, X.S.; An, Y.J.; Liu, J.; Dai, L.Q. Zircon U-Pb geochronology of the volcanic rocks from Fanchang-Ningwu volcanic basins in the Lower Yangtze region and its geological implications. *Chin. Sci. Bull.* **2009**, *54*, 2895–2904. [CrossRef]
136. Li, S.G. Infrastructure of Mesozoic magmatic rocks and copper-iron metallogenic belt in the middle and lower Yangtze river reaches. *Geol. Anhui* **2001**, *11*, 118–122, (In Chinese with English abstract).
137. Xie, G.Q.; Mao, J.W.; Hu, R.Z.; Li, R.L.; Cao, J.J. Discussion on some problems of Mesozoic and Cenozoic geodynamics of southeastern China. *Geol. Rev.* **2005**, *51*, 613–620, (In Chinese with English abstract).

138. Yan, J.; Chen, J.F.; Xie, Z.; Yang, G.; Yu, G.; Qian, H. Geochemistry of late Mesozoic from Kedoushan in the middle and lower Yangtze regions: Constrains on characteristics and evolution of the lithospheric mantle. *Geochimica* **2005**, *34*, 455–469, (In Chinese with English abstract).
139. Yuan, F.; Zhou, T.F.; Fan, Y.; Lu, S.M.; Qian, C.C.; Zhang, L.J.; Duan, C.; Tang, M.H. Source, evolution and tectonic setting of Mesozoic volcanic rocks in Luzong basin, Anhui province. *Acta Petrol. Sin.* **2008**, *24*, 1691–1702, (In Chinese with English abstract).
140. Xu, X.C.; Xu, X.Y.; Xie, Q.Q.; Fu, Z.Y.; Qian, S.L.; Xie, Z.J. Geological and geochemical characteristics and genesis of the Chating copper-gold deposit in Xuancheng City. *Acta Petrol. Sin.* **2019**, *35*, 3659–3676, (In Chinese with English abstract).
141. Zhao, X.F.; Ceng, L.P.; Liao, W.; Li, W.T.; Hu, H.; Li, J.W. An overview of recent advances in porphyrite iron (iron oxide-apatite, IOA) deposits in the Middle-Lower Yangtze River Valley metallogenic belt and its implication for ore genesis. *Earth Sci. Front.* **2020**, *27*, 197–217, (In Chinese with English abstract).
142. Yang, R.Y.; Ren, Q.J.; Xu, Z.W.; Sun, Y.D.; Guo, G.Z. The magma source of Bajiatan volcanic-intrusive complex in the Lujiang-Zongyang area, Anhui province. *Geochimica* **1993**, *22*, 197–206, (In Chinese with English abstract).
143. Zhao, B.; Xing, F.M.; Zhu, C.M.; Zhao, J.S.; Cai, E.Z.; Xu, X. Study on genesis of magma forming intermediate and intermediate-acid magmatic rocks from middle-lower reaches of Changjiang river and copper mineralization. *Geochimica* **1996**, *25*, 387–400, (In Chinese with English abstract).
144. Xing, F.M.; Zhao, B.; Xu, X.; Zhu, C.M.; Zhao, J.S.; Cai, E.Z. Experiment study on the genesis of intrusive rocks in the Tongling area, Anhui. *Reginal Geol. China* **1997**, *16*, 267–274, (In Chinese with English abstract).
145. Wang, Y.L.; Zhang, Q.; Wang, Y. Geochemical characteristics of volcanic rocks from Ningwu area, and its significance. *Acta Petrol. Sin.* **2001**, *17*, 565–575, (In Chinese with English abstract).
146. Qin, X.L. Studies on Sulfide-Metal Oxide Inclusions from Mesozoic Intrusions and Their Rock Xenoliths. Ph.D. Thesis, China University of Geosciences (Beijing), Beijing, China, 2007; pp. 1–158, (In Chinese with English abstract).
147. Yu, J.J.; Mao, J.W.; Zhang, C.Q. Evidence of mantle participation in the mineralization of Ningwu porphyrite-like rocks in Ningwu basin-from C and Sr isotope. *Prog. Nat. Sci.* **2007**, *17*, 1216–1221, (In Chinese with English abstract).
148. Pearce, J.A. *Trace Element Characteristics of Lavas from Destructive Plate Boundaries*; Chichester: Wiley, UK, 1982; pp. 525–547.
149. Middlemost, E.A.K. Naming materials in the magma/igneous rock system. *Earth Sci. Rev.* **1994**, *37*, 215–224. [CrossRef]
150. Sun, S.S.; McDonough, W.F. Chemical and Isotopic Systematics of Oceanic Basalts: Implications for Mantle Composition and Processes. *Geol. Soc. Lond. Spec. Publ.* **1989**, *42*, 313–345. [CrossRef]
151. Rudnick, R.L.; Gao, S. Composition of the continental crust. In *Treatise on Geochemistry*; Elsevier: Oxford, UK, 2004; Volume 3, pp. 1–64.
152. Janoušek, V.; Finger, F.; Roberts, M.; Fryda, J.; Pin, C.; Dolejš, D. Deciphering the petrogenesis of deeply buried granites: Whole-rock geochemical constraints on the origin of largely undepleted felsic granulites from the Moldanubian Zone of the Bohemian Massif. *Earth Environ. Sci. Trans. R. Soc. Edinb.* **2004**, *95*, 141–159. [CrossRef]
153. Deng, J.H. Subduction and Cu-Au Mineralization: Comparing Studies of the Early Cretaceous Volcanic Rocks and Adakitic Rocks in Luzong Basin, LYRB and Central Philippines. Ph.D. Thesis, University of Science and Technology of China, Hefei, China, 2015; pp. 1–172, (In Chinese with English abstract).
154. Zhang, S.B.; Zheng, Y.F.; Wu, Y.B.; Zhao, Z.F.; Gao, S.; Wu, F.Y. Zircon isotope evidence for ≥3.5Ga continental crust in the Yangtze craton of China. *Precambrian Res.* **2006**, *146*, 16–34. [CrossRef]
155. Zhang, S.B.; Zheng, Y.F.; Wu, Y.B.; Zhao, Z.F.; Gao, S.; Wu, F.Y. Zircon U-Pb age and Hf-O isotope evidence for Paleoproterozoic metamorphic event in South China. *Precambrian Res.* **2006**, *151*, 265–288. [CrossRef]
156. Zhang, S.B.; Zheng, Y.F.; Wu, Y.B.; Zhao, Z.F.; Gao, S.; Wu, F.Y. Zircon U-Pb age and Hf isotope evidence for 3.8 Ga crustal remnant and episodic reworking of Archean crust in South China. *Earth Planet. Sci. Lett.* **2006**, *252*, 56–71. [CrossRef]
157. Xia, J.L.; Huang, G.C.; Ding, L.X.; Wu, C.X.; Zhu, J.M.; Jin, S.G. Paleoproterozoic-Archean basement beneath southeast Hubei Province: Evidence from U-Pb-Hf isotopes in zircons from the Tonggushan pluton. *Acta Geosci. Sin.* **2013**, *34*, 691–701, (In Chinese with English abstract).
158. Hofmann, A.W. Sampling Mantle Heterogeneity through Oceanic Basalts: Isotopes and Trace Elements. *Treatise Geochem.* **2003**, *2*, 568.
159. Plank, T.; Langmuir, C.H.; Albarede, F.; Blicherttoft, J.; Staudigel, H.; White, W.M. The chemical composition of subducting sediment and its consequences for the crust and mantle. *Chem. Geol.* **1998**, *145*, 325–394. [CrossRef]
160. Chen, J.F.; Yan, J.; Xie, Z.; Xu, X.; Xing, F. Nd and Sr isotopic compositions of igneous rocks from the Lower Yangtze region in eastern China: Constraints on sources. *Phys. Chem. Earth Part A Solid Earth Geod.* **2001**, *26*, 719–731. [CrossRef]
161. Jahn, B.M.; Wu, F.Y.; Lo, C.H.; Tsai, C.H. Crust-mantle interaction induced by deep subduction of the continental crust: Geochemical and Sr-Nd isotopic evidence from post-collision mafic-ultramafic intrusions of the northern Dabie complex, central China. *Chem. Geol.* **1999**, *157*, 119–146. [CrossRef]
162. Wu, R.X.; Zheng, Y.F.; Wu, Y.B.; Zhao, Z.F.; Zhang, S.B.; Liu, X.M.; Wu, F.Y. Reworking of juvenile crust: Element and isotope evidence from Neoproterozoic granodiorite in South China. *Precambrian Res.* **2006**, *146*, 179–212. [CrossRef]
163. Wang, X.L.; Zhou, J.C.; Wan, Y.S.; Kitajima, K.; Wang, D.; Bonamici, C.; Qiu, J.S.; Sun, T. Magmatic evolution and crustal recycling for Neoproterozoic strongly peraluminous granitoids from southern China: Hf and O isotopes in zircon. *Earth Planet. Sci. Lett.* **2013**, *366*, 71–82. [CrossRef]

164. Xu, G.J.; Lin, X.D. An investigation into the genesis of the Changlongshan skarn-magma type of iron deposit, Anhui province. *Earth Sci.-J. China Univ. Geosci.* **1990**, *15*, 649–656+722, (In Chinese with English abstract).
165. Ren, G.L.; Wang, H.; Liu, J.P.; Wang, B.; Wu, Y.F.; Huang, C.Y. Geochemical characteristics and genesis of Taochong iron deposit in Fanchang District, Anhui Province, China. *Earth Sci. Front.* **2012**, *19*, 82–95, (In Chinese with English abstract).
166. Li, S.H. *Summary Report of Geological Survey of Suishan Zinc Mine, Fanchang County, Anhui Province*; Team of Geological Bureau: Fanchang, China, 1960; pp. 1–200.
167. Lin, S.Z. A contribution to the chemistry, origin and evolution of magnetite. *Acta Mineral. Sin.* **1982**, *3*, 166–174, (In Chinese with English abstract).
168. Zhang, L.G. *Application of Stable Isotopes in Geology*; Science and Technology Press of Shaanxi: Xi'an, China, 1985; pp. 1–267.
169. Zhou, T.F.; Yue, S.C. Isotope geochemistry of copper mineralization in Yueshan, Anhui. *Miner. Depos.* **1996**, *15*, 54–63, (In Chinese with English abstract).
170. Shmulovich, K.I.; Landwehr, D.; Simon, K.; Heinrich, W. Stable isotope fractionation between liquid and vapor in water-salt systems up to 600 °C. *Chem. Geol.* **1999**, *157*, 343–354. [CrossRef]
171. Rye, R.O.; Ohmoto, H. Sulfur and carbon isotopes and ore genesis: A review. *Econ. Geol.* **1974**, *69*, 826–842. [CrossRef]
172. Zhai, Y.S.; Yao, S.Z.; Cai, K.Q. *Mineralogy*; Geological Publishing House: Beijing, China, 2011; pp. 1–101.
173. Jiao, Y.L.; Wang, Y. Relationship between the hard-soft acid-base properties of magmatic hydrothermal and the metal metallogenic specificity. *J. Earth Sci. Environ.* **2014**, *36*, 83–93, (In Chinese with English abstract).
174. Yao, H.Z.; Yan, J.; Liu, X.Q.; Liu, J.M.; Li, Q.Z. Characteristics of oxygen fugacity of the late Mesozoic magmatic rocks in the middle-lower Yangtze River Belt and its significance. *Chin. J. Geol.* **2016**, *51*, 1163–1180, (In Chinese with English abstract).
175. Zhou, T.F.; Wang, B.; Fan, Y.; Yuan, F.; Zhang, L.J.; Zhong, G.X. Apatite-actinolite-magnetite deposit related to A-type granite in Luzong basin: Evidence from Makou iron deposit. *Acta Petrol. Sin.* **2012**, *28*, 3087–3098, (In Chinese with English abstract).
176. Liu, H.H. Study on geological characteristics of uranium mineralization and control factors in Huangmeijian area, Anhui Province. *J. East China Inst. Technol. Nat. Sci.* **2014**, *37*, 150–157, (In Chinese with English abstract).
177. Zhang, S.; Wu, M.; Wang, J.; Li, X.D.; Zhao, W.G.; Wei, G.H. The mineralization related with the syenite in Luzong Basin, Anhui Province. *Acta Geol. Sin.* **2014**, *88*, 519–531, (In Chinese with English abstract).
178. Deng, G.R. A brief analysis of geological features of the Dalongshan uranium ore deposit. *Geol. Anhui* **2017**, *27*, 95–98, (In Chinese with English abstract).
179. Zhang, D.Y.; Meng, X.; Ren, K.D.; Chen, X.F.; Ye, L.X.; Xiong, Z.Y. Mineralogy, temporal and spatial distribution of Mo mineralization in Guilinzheng Mo-W deposit, Jiangnan W mineralization belt and its significance. *Acta Petrol. Sin.* **2021**, *37*, 2821–2842, (In Chinese with English abstract).
180. Zhang, W.Z.; Wang, H.N.; Wang, M.Y. *Coordination and its Application in Geology*; Geological Publishing House: Beijing, China, 1987; pp. 1–429.
181. Wang, J.M.; Yang, N.Q.; Li, K.Q.; Ding, G.X. The metallogenesis and magmatic differentiation of Suzhou A-type granite. *Acta Petrol. Sin.* **1993**, *9*, 33–43, (In Chinese with English abstract).
182. Aylett, B.J. Group IIB. In *Comprehensive Inorganic Chemistry*; Pergamon Press: Oxford, UK, 1973.
183. Cotton, F.A.; Wilkinson, G. *Advanced Inorganic Chemistry*; John Wiley Interscience: New York, NY, USA, 1980; pp. 1–1170.
184. Schwartz, M.O. Cadmium in Zinc Deposits: Economic Geology of a Polluting Element. *Int. Geol. Rev.* **2000**, *42*, 445–469. [CrossRef]
185. Ye, L.; Pan, Z.P.; Li, C.Y.; Liu, T.G.; Xia, B. The present situation and prospects of geochemical researches on cadmium. *Acta Petrol. Et Mineral.* **2005**, *24*, 339–348, (In Chinese with English abstract).
186. Zhou, J.X.; Huang, Z.L.; Zhou, G.F.; Li, X.B.; Ding, W.; Bao, G.P. Trace elements and rare earth elements of sulfide minerals in the Tianqiao Pb-Zn ore deposit, Guizhou Province, China. *Acta Geol. Sin.-Engl. Ed.* **2011**, *85*, 189–199.
187. Fontboté, L.; Kouzmanov, K.; Chiaradia, M.; Pokrovski, G.S. Sulfide Minerals in Hydrothermal Deposits. *Elements* **2017**, *13*, 97–103. [CrossRef]
188. Chu, X.K.; Li, B.; Shen, P.; Zha, Z.H.; Lei, Z.; Wang, X.F.; Tao, S.Y.; Hu, Q. Trace elements in sulfide minerals from the Huangshaping copper-polymetallic deposit, Hunan, China: Ore genesis and element occurrence. *Ore Geol. Rev.* **2022**, *144*, 104867. [CrossRef]
189. Maruyama, S.; Isozaki, Y.; Kimura, G.; Terabayashi, M. Paleogeographic maps of the Japanese Islands: Plate tectonic synthesis from 750 Ma to the present. *Isl. Arc* **1997**, *6*, 121–142. [CrossRef]
190. Wang, Y.; Deng, J.F.; Ji, G.Y. A perspective on the geotectonic setting of early Cretaceous adakite-like rocks in the Lower Reaches of Yangtze River and its significance for copper-gold mineralization. *Acta Petrol. Sin.* **2004**, *20*, 297–314, (In Chinese with English abstract).
191. Sun, W.D.; Ding, X.; Hu, Y.H.; Li, X.H. The golden transformation of the Cretaceous plate subduction in the west Pacific. *Earth Planet Sci. Lett.* **2007**, *262*, 533–542. [CrossRef]
192. Sun, W.D.; Ling, M.X.; Yang, X.Y.; Fan, W.M.; Ding, X.; Liang, H.Y. Oceanic ridge subduction and porphyry copper-gold mineralization. *Sci. China Ser. D* **2010**, *40*, 127–137, (In Chinese with English abstract).

193. Cai, B.J. The relationship of gypsum salt beds with endogenic copper and iron ores in the middle-lower Yangtze Valley. *Geochimica* **1980**, *9*, 193–199, (In Chinese with English abstract).
194. Hu, L.; Zhang, D.X.; Lou, W.; Hu, Z.Q.; Liu, J.B. In situ LA-ICP-MS determination of trace elements in magnetite from a gypsum-salt bearing iron deposit and geochemical characteristics. *Rock Miner. Anal.* **2022**, *41*, 564–574.